DISSERTATION

PHYSICAL PROPERTIES OF POROUS MEDIUM AFFECTING LAMINAR AND TURBULENT FLOW OF WATER

Submitted by

Nazeer Ahmed

In partial fulfillment of the requirements
for the degree of Doctor of Philosophy
in Civil Engineering
Colorado State University
Fort Collins, Colorado
June 1967

COLORADO STATE UNIVERSITY

June 8 1967

WE HEREBY RECOMMEND THAT THE DISSERTATION PREPARED UNDER OUR SUPERVISION BY

Nazeer Ahmed

ENTITLED PHYSICAL PROPERTIES OF POROUS MEDIUM AFFECTING LAMINAR AND TURBULENT FLOW OF WATER

BE ACCEPTED AS FULFILLING THIS PART OF THE REQUIREMENTS FOR THE DEGREE OF DOCTOR OF PHILOSOPHY

Committee on Graduate Work

Major Professor

Wm Doral Kemper

Morton W. Bettinger

Head of Department

Examination Satisfactory

Committee on Final Examination

Wm Doral Kemper

Morton W. Bettinger

Chairman

Permission to publish this dissertation or any part of it must be obtained from the Dean of the Graduate School.

"Dedicated with respect to my parents"

ABSTRACT OF DISSERTATION

An investigation was conducted to study the influences of certain physical properties of the porous medium on the flow phenomena. An equation, representing hydraulic gradient as a function of bulk velocity, was developed by analyzing the Navier-Stokes equations. During the development of the equation it was shown that energy losses caused by turbulence being small could be neglected in comparison to the energy represented by convective terms.

Two dimensionless parameters were developed from the flow equation, and a unique relationship was shown to exist between them for all porous media studied in this investigation.

The characteristic length of the flow was shown to have linear relationships with particle diameter obtained from sieve analysis, and pore and grain diameter obtained from cut-section data of porous media.

Nazeer Ahmed
Civil Engineering Department
Colorado State University
Fort Collins, Colorado
June 1967

ACKNOWLEDGMENTS

The author wishes to express sincere thanks and appreciation to his major professor, Dr. Daniel K. Sunada, Assistant Professor of Civil Engineering, for his guidance during the course of this study. His continuous encouragement as well as his valuable suggestions and contributions have made this dissertation possible.

The author's research and dissertation committee, Dr. William D. Kemper, Associate Professor of Soil Science; Morton W. Bittinger, Associate Professor of Civil Engineering; Dr. Donald P. Squier, Associate Professor of Mathematics; and Robert A. Longenbaugh, Assistant Professor of Civil Engineering, reviewed and had many valuable comments on the dissertation.

Jack R. Chitwood aided in the design of the experimental apparatus and Ralph Asmus and his crew helped with its construction and installation.

Helpful suggestions of Harold R. Duke are greatly appreciated. Miss Hanae Akari traced the figures; rough and final draft of the dissertation were typed in the steno pool by Miss Kathleen Wood and Mrs. Joella Matthews; Duayne Barnhardt prepared the photographs of cut-sections. Help is acknowledged of the Geology Department for allowing the use of their diamond cutter. Finally, financial assistance of the National Science Foundation, under Grant No. GK-1162 is acknowledged and greatly appreciated.

TABLE OF CONTENTS

TABLE OF CONTENTS - Continued

LIST OF TABLES

LIST OF FIGURES

Chapter I

INTRODUCTION

The relationship between flow rate and pressure gradient is represented by Darcy's empirical formula for laminar flow through porous media. For non-linear flow through porous media, the Navier-Stokes equations can be solved for pressure gradient in terms of flow velocity, fluid properties, and porous medium properties. The geometric properties of porous medium are represented by the constant c, which is related to the permeability k of porous medium as

$$c = \frac{k}{d^2} \tag{1}$$

where d is a characteristic length of the flow.

Many investigations have been conducted toward evaluating the relationship given by equation 1. Previous investigators (2, 3, 4, 5, 10, 11, 17, 30)* have assumed that the characteristic length can be represented by the particle size. These investigators obtained excellent relationships between particle size and permeability for their data. However, the results obtained by one investigator cannot, in general, be applied to those obtained by others. The discrepancy results from

---

* Numbers in parenthesis refer to the numbers in the bibliography.

the arbitrary definition of the particle size and the absence of appropriate experimental techniques for the evaluation of the constant c .

Sunada (35) has shown that the constant c can be evaluated from data of hydraulic gradient and flow velocities providing that the effects of turbulence on the flow are relatively minor compared to the effects of convective forces for non-linear flow. If the constant c can be evaluated, then it should be possible to relate d to some measurable length of the porous medium. The goals of the present investigation are:

1. To establish the relative importance of turbulent and convective losses.
2. To evaluate the product cd^2 , and the terms c and d from hydraulic measurements of the flow through porous media.
3. To find mathematical and experimental correlation between d from hydraulic measurements, d from statistical analyses of cut sections, and sieve size analysis.

The experimental procedure for hydraulic measurements consisted of measurements of gradient and bulk flow velocities for six porous media for the present investigation. The measurement of the microscopic velocities with an electro-kinetic probe proved unsuccessful due to excessive noise generated by the various equipment in the hydraulics laboratory and stray signals present in the atmosphere.

The signal generated by the flow itself (approximately five to ten percent of the total signal), although detectable, could not be analyzed because of inconsistencies in the signal output. A procedure is needed whereby stray signals could be eliminated or suppressed.

Statistical analysis consisited of measuring pore diameter, grain diameter, and porosity from cut sections of the porous medium sample. A complete description of the experimental apparatus and procedures is given in Appendix A. In this dissertation, the diameter for sand particles obtained from sieve analysis is termed "particle diameter" and is denoted by d_s ; the diameter obtained from a cut-section of a porous medium is termed "grain diameter" and is denoted by d_g.

Chapter II

LITERATURE REVIEW

Flow characteristics in a porous medium depend upon the fluid and porous medium properties. The geometry of particles in a porous medium is quite complex and is not amenable for exact mathematical evaluation. Several investigations have been conducted to evaluate the flow phenomena in terms of the geometry of particles. In this chapter a review of different works is presented. Different flow regimes, laminar and turbulent, coupled with transitional flow are critically reviewed.

Henry Darcy (9) was among the first to investigate laminar flow through beds of filter sands. He stated the empirical relationship between flow rate and pressure gradient as "the volume rate of flow is directly proportional to the pressure drop and inversely proportional to the thickness of the bed" or mathematically

$$q = K\frac{\Delta P}{l} \tag{2}$$

where

q = volume rate of flow through the filter bed or bulk velocity,

K = constant of proportionality, usually known as Darcy's coefficient of permeability,

ΔP = pressure drop across the filter bed, and

l = thickness of filter bed.

The volume rate of flow and pressure gradient are macroscopic quantities which can be easily measured. The constant of proportionality K is affected by the fluid and porous medium properties. The properties of the fluid are density and dynamic viscosity. The properties of porous medium are geometric properties which, to date, are not measurable. It is possible to distinguish the properties of the fluid from those of porous medium and express K as a function of both fluid and porous medium properties as

$$K = \frac{\rho g}{\mu}(cd^2) \tag{3}$$

where

c = constant

d = characteristic length of flow

ρ = density of the fluid

g = acceleration of gravity

μ = dynamic viscosity of the fluid.

The product cd^2 is termed permeability of porous medium and is denoted by k.

Theoretically, laminar flow does not exist in porous media because of convective accelerations of fluid particles due to the continuous expansion and contraction of fluid channels. However, when convective accelerations are small, they may be neglected and laminar flow can be assumed without appreciable error. The Navier-Stokes equations are used to describe the hydrodynamics of laminar flow through porous media. In tensor notation they are:

$$u_j \frac{\partial u_i}{\partial x_j} = -\frac{1}{\rho}\frac{\partial p}{\partial x_i} + \frac{\mu}{\rho}\frac{\partial^2 u_i}{\partial x_j \partial x_j} \tag{4}$$

for steady, incompressible flow.

In the above equation,

u = instantaneous velocity

p = pressure at a point

x = coordinate distance

i = component, and i = 1, 2, 3

j = repeated operator, and j = 1, 2, 3

Since convective accelerations are small and can be neglected, the terms $u_j \frac{\partial u_i}{\partial x_i}$ can be set equal to zero. Consequently, equation 4 becomes

$$\frac{\partial p}{\partial x_i} = \mu \frac{\partial^2 u_i}{\partial x_j \partial x_j} \tag{5}$$

Simple solutions of equation 5 can be found in literature (6). For flow through straight circular tubes, the solution is given by the Poiseuille equation,

$$\overline{V} = -\frac{r_t^2}{8\mu}\frac{dP}{dx} \tag{6}$$

where

$\overline{V}$ = mean velocity in the cross section

r_t = radius of the tube.

Similarly, for flow over an infinite flat plate the equation is:

$$\overline{V} = -\frac{e^2}{3\mu}\frac{dP}{dx} \tag{7}$$

where

e = depth of flow over the plate.

By induction, an analogous equation applying to straight tubes of uniform cross section other than a circular section is

$$\overline{V} = -\frac{B^2}{\zeta\mu}\frac{dP}{dx} \tag{8}$$

where

B = a length parameter characterizing the size of the tube

ζ = a shape factor depending upon the cross section of the tube.

Kozeny (18) made use of equation 8 but modified various terms to include the effects of porosity and irregularity of flow channels. For the length B he substituted the hydraulic radius which is defined as the ratio of volume of fluid divided by the wetted surface in the flow system. His equation of pressure gradient for flow through porous media is

$$\frac{\Delta P}{l_e} = 2\mu\frac{q}{\epsilon}\left(\frac{A_g}{V_g}\right)^2\frac{(1-\epsilon)^2}{\epsilon^3} \tag{9}$$

where

l_e = the average tortuous length a fluid element actually travels in a porous medium of thickness l

ϵ = porosity

A_g = surface area of grains of porous media

V_g = volume of grains.

In Kozeny's equation the number "2" represents the value of shape factor ζ for a circular cross section.

Fair and Hatch (11) developed an equation similar to equation 9 by using pipe flow formula and introducing appropriate changes in different parameters. Carman (5) noted that Kozeny's shape factor for various cross sections has a value between two and three. During an experiment for flow through granular material he injected dye and observed dye filaments making an angle of 45^0 with the macroscopic flow direction. He thus concluded that it was reasonable to take $\frac{l_e}{l} = \sqrt{2}$. He also noted that the average pore velocity would be $\frac{q}{\epsilon} \frac{l_e}{l}$, and not $\frac{q}{\epsilon}$ as Kozeny postulated. He gave his final equation as

$$\frac{\Delta P}{l} = 5 \mu q \left(\frac{A_g}{V_g} \right)^2 \frac{(1-\epsilon)^2}{\epsilon^3} \tag{10}$$

Equation 10 is referred to as the Kozeny-Carman equation.

Sullivan (34) introduced an orientation factor θ_o, defined as the average value of the square of the size of the angle between a normal to the walls forming the microscopic flow channel and the macroscopic direction of flow. Thus, the Kozeny-Carman equation would become

$$\frac{\Delta P}{l} = 5\mu q \theta_o \left(\frac{A_g}{V_g}\right)^2 \frac{(1-\epsilon)^2}{\epsilon^3}. \tag{11}$$

Equation 11 can be written in general terms as

$$\frac{\Delta P}{l} = \left\{ \zeta \left(\frac{l_e}{l}\right)^2 \frac{\theta_o}{\xi^2} \frac{(1-\epsilon)^2}{\epsilon^3} \right\} \mu q \tag{12}$$

where

$\xi = \dfrac{V_g}{A_g}$ is a length parameter and other terms are defined as before. Though incomplete, all the factors inside the brackets represent only the properties of porous media.

Burke and Plummer (4) developed a theory based upon spherical particles and resistance to flow as encountered by each individual particle. Their final expression for pressure gradient for laminar flow is

$$\frac{\Delta P}{l} = \frac{9}{2} \frac{1-\epsilon}{\epsilon^2} \frac{1}{r_p^2} \mu q \tag{13}$$

where

r_p = radius of the particle.

Franzini (14) experimentally verified that the relationship between porosity and resistance coefficient was represented by the Fair-Hatch expression $\dfrac{(1-\epsilon)^2}{\epsilon^3}$ as the porosity function for flow in laminar regime.

Darcy's equation does not apply to non-linear and turbulent flow. As a result, investigations were conducted toward evaluating different parameters of porous media affecting the flow phenomena. Forchheimer (13) was among the first who experimentally verified the quadratic equation

$$\frac{\Delta P}{l} = a'q + b'q^2 \tag{14}$$

where a' and b' are constants which depend upon fluid and porous medium properties. Since then, expressions similar to equation 14 have been developed by many investigators. Ergun (10) has shown that for non-linear flow, the pressure gradient may be represented by

$$\frac{\Delta P}{l} = 150 \frac{(1-\epsilon)^2}{\epsilon^3} \frac{\mu q}{D^2} + 1.75 \frac{1-\epsilon}{\epsilon^3} \frac{\rho q^2}{D} \tag{15}$$

where D is the average diameter of the particles. Equation 15 can be transformed into dimensionless parameters as

$$f_v = 150 + 1.75 \frac{R_D}{1-\epsilon} \tag{16}$$

where f_v is the ratio of pressure gradient to viscous forces and R_D is the Reynolds number dependent upon particle diameter D. He presented the results of 640 experiments in a graphical plot of f_v versus $\frac{R_D}{(1-\epsilon)}$. Inspection of these curves shows that there is a smooth transition from laminar to non-linear flow.

Cornell and Katz (7) derived a similar expression for turbulent flow using Kozeny's equation. Their final expression for compressible flow is

$$\frac{\Delta P^2}{l} = \frac{32\ T_o}{\epsilon\ \zeta_1 D_p^2} \frac{2\mu z_1 R T_1 G}{m} + \frac{32\ T_o^{3/2}}{\epsilon^2 \zeta_2 D_p} \frac{2 z_1 R T_1 G^2}{m} \tag{17}$$

where

$T_o = \left(\frac{l_e}{l}\right)$ = tortuosity

ζ_1 = shape factor dependent upon pore structure

ζ_2 = correction factor

D_p = effective diameter of pore structure

R = gas constant

z_1 = compressibility factor of a gas

T_1 = absolute temperature

m = molecular weight of a gas

G = ρq = mass rate of flow.

While studying flow of compressible fluids through consolidated porous media, they showed that area available for flow is equal to the product of the total cross-sectional area, porosity, and $\frac{l_e}{l}$ or

$$A = A_t\ \epsilon\ \frac{l_e}{l} \tag{18}$$

where

A = available cross-sectional area

A_t = total cross-sectional area.

An examination of their general equation for compressible flow shows that factors ζ_1 and ζ_2 have apparently been used as correction factors to satisfy laminar and turbulent flow condition.

Blake (2) obtained two dimensionless groups, $\frac{\Delta P}{\rho q^2} \frac{D}{l} \frac{\epsilon^3}{(1-\epsilon)}$, and $\frac{D\rho q}{\mu(1-\epsilon)}$, to represent flow through porous media. The first of these groups is recognized as the modified friction factor and the second as the modified Reynolds number. Ergun suggests, since both of these groups contain porosity functions, pressure gradient is a function of both the groups.

Brownell and Katz (3) demonstrated that the dimensionless group postulated by Reynolds for conduits may be enlarged by including other variables necessary to define flow through porous media. They define the Reynolds number as

$$R_\epsilon = \frac{\rho q D}{\mu \, \epsilon^{m_1}} \tag{19}$$

where m_1 is an exponent dependent upon the shape of the particles and the bed porosity. They maintain that porosity of a pipe is unity and equation 19 applies to both porous media and pipes. They define friction factor, taking into consideration the porous media properties, as

$$f_\epsilon = \frac{2 D \Delta P \epsilon^{n_1}}{\rho l q^2} \tag{20}$$

where n_1 is an exponent dependent upon the shape of the particles and the bed porosity. They state that the gradual transition from laminar to turbulent flow is due to a composite of a number of flow paths, some in laminar regime and some in turbulent regime. However, they did not obtain a unique representation of f_ϵ versus R_ϵ for different porous media.

Recently, Ward (37) has derived a pressure gradient equation from dimensional analysis. The equation is given as

$$\frac{\Delta P}{l} = \frac{\mu}{k} q + \frac{0.55 \rho}{\sqrt{k}} q^2, \tag{21}$$

The constant 0.55 , is stated to be a univeral constant, applicable to all porous media. The discussions by Larsen, O'Neill and Parkin (22) and Sunada (36) seem to indicate that the value 0.55 cannot apply to all porous media. As a result, equation 21 appears to be invalid.

Irmay (17) has outlined a procedure to derive Darcy's equation and Forchheimer's equation from the Navier-Stokes equations for the case of viscous incompressible flow through a homogeneous, isotropic, and saturated media. He developed Darcy's equation as

$$\frac{\Delta P}{l} = \frac{\beta}{D^2} \frac{(1-\epsilon)^2}{\epsilon^3} \mu q \tag{22}$$

and Forchheimer's equation as

$$\frac{\Delta P}{l} = \frac{\beta}{D^2} \frac{(1-\epsilon)^2}{\epsilon^3} \mu q + \frac{\alpha (1-\epsilon)}{D \epsilon^3} \rho q^2 \tag{23}$$

where α and β are numerical shape factors dependent upon the shape of particles and the structure of porous medium.

Rumer (30) has developed Darcy's equation considering Navier-Stokes equations in dimensionless form for the laminar flow regime. He has shown that there exists a characteristic grain length D_{50} for porous media which is related to permeability as

$$k = c\, D_{50}^2 \tag{24}$$

where D_{50} is the 50% grain size of porous media.

Sunada (35), while developing functional relationship for laminar and turbulent flow through porous media from Navier-Stokes equations, has not only shown that the relationship $k = cd^2$ exists but also that the length d can be obtained from hydraulic measurements of flow through porous media. His general equation for pressure gradient of turbulent flow through porous media is

$$\frac{d\bar{p}}{dx} = \frac{\mu q}{d^2}\left[\frac{\partial^2 \bar{u}_{ri}}{\partial x_{rj}\, \partial x_{rj}}\right] + \frac{\rho q^2}{d}\left[-\bar{u}_{rj}\frac{\partial \bar{u}_{ri}}{\partial x_{rj}} - \overline{u'_{rj}\frac{\partial u'_{ri}}{\partial x_{rj}}}\right] \tag{25}$$

where

$\bar{p}$ = the time average pressure at a point

$\bar{u}$ = the time average microscopic velocity at a point

$\bar{u}_r = \frac{\bar{u}}{q}$ = dimensionless time average microscopic velocity at a point

r = a subscript, denoting a dimensionless variable

u'_r = dimensionless fluctuating microscopic velocity about the mean at a point

The terms within the square brackets were shown to be constant for a given porous medium. The final equation in the simplified form is

$$\frac{\Delta P}{l} = a'q + b'q^2 \tag{26}$$

where

$$a' = \frac{\mu}{k} , \quad \text{and} \quad b' = \frac{\rho}{\sqrt{ck}} .$$

Review of literature indicates that flow through porous media is complex and there is no analytical treatment available which could solve the geometrical problems of porous media. Efforts have been made by various investigators to incorporate the geometric properties into their respective flow equations developed for flow through porous media. Reviews of such works have been presented by Romita (28), Leva et al. (23), and Scheidegger (31). In general, there is no correlation between the results of different investigations. For example, different porosity functions, summarized by Sunada (35), have been used, and all of them seem to have worked very well for the particular medium studied. But no unique porosity function has been developed which is applicable to all porous media.

Similarly, correction factors in the form of tortuosity, shape factors, and other numerical constants have been introduced to make the equation fit the experimental data. These correction factors are not universal and need to be determined experimentally for each porous medium under investigation. As a result, flow equations developed are restricted in their application to all porous media and the form and magnitude of the correction factors need to be determined each time. The average diameter of particles, the average diameter of pore structure, hydraulic radius, and even the square root of permeability have been used as a length parameter to characterize the flow. No correlation has been shown between these length parameters. For non-linear flow, equations of the quadratic type have been suggested and verified experimentally provided correction factors are introduced. Again these correction factors are not universal.

Hubbert (16) and Schneebeli (33) believe the initial departure from linearity is due to the convective accelerations. Irmay (17) points out the fact that the kinetic energy losses are not necessarily due to turbulence but may be due to the emergence of inertia effects in laminar flow.

Sunada's theoretical analysis has shown the separability of hydrodynamical and geometrical effects on the pressure gradient for flow through porous media. Individual geometrical factors have not been elaborated because they cannot be expressed mathematically for a unique relationship.

Krumbein and Monk (21) made a systematic investigation for the effects of grain-size distribution on the permeability. They conclude that it is possible to change the permeability, keeping the mean diameter constant, and changing only the standard deviation of the grain size. Consequently, for this study, the porous medium was selected from grain diameter of approximately the same size. Six samples having different diameters were used. For details see Appendix A.

Chapter III

THEORETICAL CONSIDERATIONS AND PRESENTATION AND DISCUSSION OF DATA

The analysis presented in this chapter is divided into two sections. Section 1 deals with the development of an equation relating the hydraulic gradient to the macroscopic flow velocity by analyzing the Navier-Stokes equations in dimensionless form. The analysis takes into consideration the following assumptions.

1. The macroscopic properties of porous media are homogeneous and isotropic.
2. The fluid is incompressible and the media is fully saturated with the fluid used in the experiment.
3. Thermodynamic and chemical effects are small.

Pressure gradient is shown to be represented by the hydrodynamics of flow and the geometric properties of porous media. Relative importance of shear, convective, and turbulent stresses is discussed in the pressure gradient equation. Also, it is shown that energy dissipated by turbulence is small compared to the energy represented by convection. Finally, the equation of flow developed in this section is put in the form of two dimensionless parameters representing flow behavior through all porous media. Their unique relationship is verified experimentally.

Section 2 describes a statistical procedure relating the characteristic length d , and the average diameter d_s of particles obtained from a sieve analysis. This development is based upon uniform sized porous media and the experimental correlation of d versus d_s is presented in a systematic manner.

Section 1. Development and Verification of an Equation Relating Hydraulic Gradient and Bulk Velocity

The simplified form of Navier-Stokes equations for incompressible fluids and steady state flow without body forces is (35)

$$u_j \frac{\partial u_i}{\partial x_j} = -\frac{1}{\rho}\frac{\partial p}{\partial x_i} + \frac{\mu}{\rho}\frac{\partial^2 u_i}{\partial x_j \partial x_j} \tag{4}$$

where all the terms in the above equation have been defined before. Sunada has used Navier-Stokes equations in dimensionless form for laminar and turbulent flow through porous media. He has replaced instantaneous quantities of velocities and pressures by an average and a fluctuating component, such as:

$$u = \bar{u} + u' , \quad \text{and} \quad p = \bar{p} + p' \quad .$$

The various terms in the Navier-Stokes equations can be made dimensionless by

$$u_r = \frac{u}{q} , \quad x_r = \frac{x}{d} \quad \text{and} \quad p_r = \frac{p}{\rho q^2} \quad .$$

The Navier-Stokes equations may now be written in dimensionless form as:

$$\frac{q^2}{d}\left[\left(\bar{u}_{rj} + u'_{rj}\right)\left(\frac{\partial(\bar{u} + u')_{ri}}{\partial x_{rj}}\right)\right] = -\frac{q^2}{d}\left[\frac{\partial(\bar{p} + p')_{r}}{\partial x_{ri}}\right] + \frac{\mu q}{\rho d^2}\left[\frac{\partial^2(\bar{u} + u')_{ri}}{\partial x_{rj}\,\partial x_{rj}}\right] \tag{27}$$

Taking the time average of all the terms and solving for $\frac{\partial \bar{p}}{\partial x_i}$, equation 27 becomes

$$\frac{\partial \bar{p}}{\partial x_i} = \frac{\mu q}{d^2}\left(\frac{\partial^2 \bar{u}_{ri}}{\partial x_{rj}\,\partial x_{rj}}\right) + \frac{\rho q^2}{d}\left(-\bar{u}_{rj}\frac{\partial \bar{u}_{ri}}{\partial x_{rj}} - \overline{u'_{rj}\frac{\partial u'_{ri}}{\partial x_{rj}}}\right) \tag{28}$$

The terms $\frac{\partial \bar{p}}{\partial x_i}$ are the time average pressure gradients in different directions at a point. At successive sections perpendicular to the direction of macroscopic flow the sum of $\frac{\partial \bar{p}}{\partial x_i}$ has a definite value in the direction of the macroscopic flow. In the other two co-ordinate directions $\frac{\partial \bar{p}}{\partial x_i}$ add up to zero because of the microscopic and macroscopic boundary conditions. Thus, the volume integration of $\frac{\partial \bar{p}}{\partial x_i}$ will have a definite value in the direction of macroscopic flow but will have zero values in the other two directions. The volume integral of the pressure gradient is

$$\iiint_{(\epsilon V)} \frac{\partial \bar{p}}{\partial x_i}(\epsilon\, dV) = \iiint_{(\epsilon V)} \left(\frac{\partial \bar{p}}{\partial x}\vec{I}_1 + \frac{\partial \bar{p}}{\partial y}\vec{I}_2 + \frac{\partial \bar{p}}{\partial z}\vec{I}_3\right)(\epsilon\, dV)$$

$$= \iiint_{(\epsilon V)} \frac{\partial \bar{p}}{\partial x}(\epsilon\, dV)\vec{I}_1 + \iiint_{(\epsilon V)} \frac{\partial \bar{p}}{\partial y}(\epsilon\, dV)\vec{I}_2 + \iiint_{(\epsilon V)} \frac{\partial \bar{p}}{\partial z}(\epsilon\, dV)\vec{I}_3 \tag{29}$$

where V = bulk volume of porous media and $\vec{I}_1$, $\vec{I}_2$, and $\vec{I}_3$ are unit vectors in x , y , and z directions, respectively.

The space average pressure gradients in the three co-ordinate directions are defined as

$$\frac{dP}{dx} = \frac{1}{\epsilon V} \iiint_{(\epsilon V)} \frac{\partial \bar{p}}{\partial x} (\epsilon\, dV) \qquad (30)$$

$$\frac{dP}{dy} = \frac{1}{\epsilon V} \iiint_{(\epsilon V)} \frac{\partial \bar{p}}{\partial y} (\epsilon\, dV) \qquad (31)$$

$$\frac{dP}{dz} = \frac{1}{\epsilon V} \iiint_{(\epsilon V)} \frac{\partial \bar{p}}{\partial z} (\epsilon\, dV) \qquad (32)$$

Next, it is shown that $\frac{dP}{dy} = \frac{dP}{dz} = 0$ and $\frac{dP}{dx} \neq 0$ by evaluating the volume integrals of $\frac{\partial \bar{p}}{\partial x_i}$ for the three co-ordinate directions.

$$\iiint_{(\epsilon V)} \frac{\partial \bar{p}}{\partial x_i} (\epsilon\, dV) =$$

$$\iiint_{(\epsilon V)} \left[\frac{\mu q}{d^2} \frac{\partial^2 \bar{u}_{ri}}{\partial x_{rj}\, \partial x_{rj}} + \frac{\rho q^2}{d} \left(-\bar{u}_{rj} \frac{\partial \bar{u}_{ri}}{\partial x_{rj}} - \overline{u'_{rj} \frac{\partial u'_{ri}}{\partial x_{rj}}} \right) \right] (\epsilon\, dV) =$$

$$\frac{\mu q}{d^2} \iiint_{(\epsilon V)} \frac{\partial^2 \bar{u}_{ri}}{\partial x_{rj}\, \partial x_{rj}} (\epsilon\, dV) - \frac{\rho q^2}{d} \iiint_{(\epsilon V)} \bar{u}_{rj} \frac{\partial \bar{u}_{ri}}{\partial x_{rj}} (\epsilon\, dV) - \frac{\rho q^2}{d} \iiint_{(\epsilon V)} \overline{u'_{rj} \frac{\partial u'_{ri}}{\partial x_{rj}}} (\epsilon\, dV). \qquad (33)$$

The volume integration of each part on the right hand side of equation 33 can be evaluated separately. The first term on the right hand side of equation 33 is

$$\frac{\mu q}{d^2} \iiint_{(\epsilon V)} \frac{\partial^2 \bar{u}_{ri}}{\partial x_{rj} \partial x_{rj}} (\epsilon\, dV) = \frac{\mu q}{d^2} \iiint_{(\epsilon V)} \nabla^2_{rj} \bar{u}_{ri} (\epsilon\, dV)$$

$$= \frac{\mu q}{d^2} \iiint_{(\epsilon V)} \left[\nabla_{rj} (\nabla_{rj} \cdot \bar{u}_{ri}) - \nabla_{rj} \times \nabla_{rj} \times \bar{u}_{ri} \right] (\epsilon\, dV) \quad .$$

Now, $\nabla_{rj} \cdot \bar{u}_{ri} = 0$ because the fluid is assumed to be incompressible. Therefore,

$$\frac{\mu q}{d^2} \iiint_{(\epsilon V)} \frac{\partial^2 \bar{u}_{ri}}{\partial x_{rj} \partial x_{rj}} (\epsilon\, dV) = \frac{\mu q}{d^2} \iiint_{(\epsilon V)} \left(- \nabla_{rj} \times \nabla_{rj} \times \bar{u}_{ri} \right) (\epsilon\, dV)$$

$$= - \frac{\mu q}{d^2} \iint_{(\epsilon S)} \vec{n} \times (\nabla_{rj} \times \bar{u}_{ri}) \;\; \epsilon\, dS ,$$

Consider the body of porous medium shown in Figure 1. The surface integration can be evaluated easily. The surface integration of S_3 which comprises of macroscopic and microscopic surfaces is zero because $\vec{n} \times (\nabla_{rj} \times \bar{u}_{ri}) = 0$ everywhere on S_3. However, for surfaces S_1 and S_2, $\vec{n} \times (\nabla_{rj} \times \bar{u}_{ri})$ does not vanish identically.

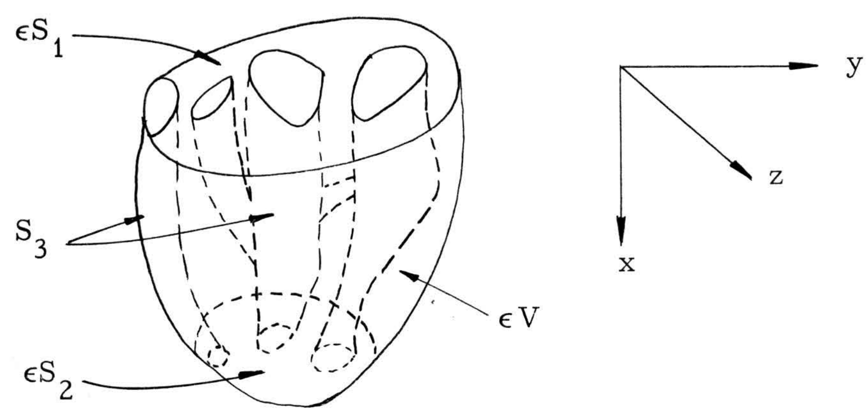

Figure 1. Arbitrary body of a porous medium

Take the surface S_1 first and evaluate the integral on this surface.

For x-direction:

The vorticity vector $\nabla_{rj} \times \bar{u}_{ri}$ is parallel to the surface S_1, and when crossed with unit normal vector $\vec{n}$ is transformed into a new vorticity vector lying on the surface and still parallel to it. It varies in magnitude in the direction of $\vec{n}$, or the macroscopic flow direction x, and produces shear losses.

For y and z-directions:

The vorticity vector $\nabla_{rj} \times \bar{u}_{ri}$ is perpendicular to the surface S_1 and, when crossed with unit normal vector $\vec{n}$, becomes identically equal to zero and thus contributes nothing to shear losses.

Similarly, for the surface S_2 shear losses do occur in the x-direction and there is no contribution in the y and z-directions. Thus, when the volume is reduced to infinitely small thin layer, the shear loss will produce pressure drop only in the x-direction. The second term of equation 33 is

$$\frac{\rho q^2}{d} \iiint_{(\epsilon V)} \bar{u}_{rj} \frac{\partial \bar{u}_{ri}}{\partial x_{rj}} (\epsilon\, dV) = \frac{\rho q^2}{d} \iiint_{(\epsilon V)} \left(\bar{u}_{rj} \cdot \nabla_{rj}\right) \bar{u}_{ri} (\epsilon\, dV)$$

$$= \frac{\rho q^2}{d} \iiint_{(\epsilon V)} \left[\nabla_{rj} \cdot \left(\bar{u}_{rj} \bar{u}_{ri}\right) - u_{rj}\left(\nabla_{rj} \cdot \bar{u}_{ri}\right)\right] (\epsilon\, dV) \quad .$$

But $\nabla_{rj} \cdot \bar{u}_{ri} = 0$ because of incompressibility. Therefore,

$$\frac{\rho q^2}{d} \iiint_{(\epsilon V)} \bar{u}_{rj} \frac{\partial \bar{u}_{ri}}{\partial x_{rj}} (\epsilon\, dV) = \frac{\rho q^2}{d} \iiint_{(\epsilon V)} \nabla_{rj} \cdot \left(\bar{u}_{rj} \bar{u}_{ri} \right) (\epsilon dV)$$

$$= \frac{\rho q^2}{d} \iint_{(\epsilon S)} \vec{n} \cdot \left(\bar{u}_{rj} \bar{u}_{ri} \right) (\epsilon\, dS).$$

The surface integral on the right-hand side can now be interpreted as follows. At the surface S_3, its value is identically equal to zero because there is no momentum transfer perpendicular to S_3. At the surfaces S_1 and S_2 there is no projection of $\vec{n}$ in y and z-directions and, hence, no momentum transfer in those directions. The integral, however, does have a definite value in the x-direction because of the momentum transfer.

The procedure for the evaluation of volume integral of the second term shows that the third term

$$\frac{\rho q^2}{d} \iiint_{(\epsilon V)} \overline{u'_{rj} \frac{\partial u'_{ri}}{\partial x_{rj}}} (\epsilon\, dV) = \overline{\frac{\rho q^2}{d} \iiint_{(\epsilon V)} u'_{rj} \frac{\partial u'_{ri}}{\partial x_{rj}} (\epsilon\, dV)}$$

vanishes in the y and z-directions but it does have a definite value in the macroscopic flow direction.

Therefore,

$$\frac{dP}{dy} = 0 \tag{34}$$

$$\frac{dP}{dz} = 0 \tag{35}$$

$$\frac{dP}{dx} \neq 0 \tag{36}$$

and

$$\frac{dP}{dx} \equiv \frac{1}{\epsilon V} \iiint_{(\epsilon V)} \frac{\partial \bar{p}}{\partial x_i} \, (\epsilon \, dV) \tag{37}$$

Therefore, the space average pressure gradient becomes

$$\frac{dP}{dx} = \frac{1}{\epsilon V} \iiint_{(\epsilon V)} \left[\frac{\mu q}{d^2} \left(\frac{\partial^2 \bar{u}_{ri}}{\partial x_{rj} \, \partial x_{rj}} \right) + \frac{\rho q^2}{d} \left(- \bar{u}_{rj} \frac{\partial \bar{u}_{ri}}{\partial x_{rj}} - \overline{u'_{rj} \frac{\partial u'_{ri}}{\partial x_{rj}}} \right) \right] (\epsilon \, dV) =$$

$$\frac{1}{\epsilon V} \frac{\mu q}{d^2} \iiint_{(\epsilon V)} \frac{\partial^2 \bar{u}_{ri}}{\partial x_{rj} \, \partial x_{rj}} (\epsilon \, dV) + \frac{1}{\epsilon V} \frac{\rho q^2}{d} \iiint_{(\epsilon V)} \left(- \bar{u}_{rj} \frac{\partial \bar{u}_{ri}}{\partial x_{rj}} - \overline{u'_{rj} \frac{\partial u'_{ri}}{\partial x_{rj}}} \right) (\epsilon \, dV). \tag{38}$$

The ratio term $u_r = \frac{u}{q}$ is constant at a point for all values of q . Also, u_r has a different value at each of the points making it possible for the derivatives $\frac{\partial u_r}{\partial x_r}$ and $\frac{\partial^2 u_r}{\partial x_r^2}$ to exist at all the points. The characteristic length parameter d is constant for one porous medium. Therefore, the integral $\frac{1}{\epsilon V} \iiint_{(\epsilon V)} \left(\frac{\partial^2 \bar{u}_{ri}}{\partial x_{rj} \, \partial x_{rj}} \right) (\epsilon \, dV)$ has a constant space average value for the entire range of velocities and reflects the effects of boundary conditions of the particles in the porous medium. Similarly, the second integral

$$\frac{1}{\epsilon V} \iiint_{(\epsilon V)} \left(- \bar{u}_{rj} \frac{\partial \bar{u}_{ri}}{\partial x_{rj}} - \overline{u'_{rj} \frac{\partial u'_{ri}}{\partial x_{rj}}} \right) (\epsilon \, dV)$$

also has a constant space average value for all values of q and reflects only the effects of boundary conditions of the particles in the porous medium. These constants have only one value for one porous medium but may have different values for others.

For small values of q (i.e., $q >> q^2$), Darcy's equation 2 and equation 38 are identical and

$$\frac{dP}{dx} = \frac{\mu q}{d^2} \frac{1}{\epsilon V} \iiint_{(\epsilon V)} \frac{\partial^2 \bar{u}_{ri}}{\partial x_{rj} \partial x_{rj}} (\epsilon\, dV) = \frac{\mu}{k} q \quad .$$

Since $k = cd^2$, then

$$\frac{1}{\epsilon V} \iiint_{(\epsilon V)} \frac{\partial^2 \bar{u}_{ri}}{\partial x_{rj} \partial x_{rj}} (\epsilon\, dV) = \frac{1}{c} \quad . \tag{39}$$

The Reynolds number for flow through porous media is

$$N = \frac{\rho q d}{\mu} \tag{40}$$

By definition, the Reynolds number is also

$$N = \frac{\text{Inertia force}}{\text{Viscous force}}$$

or

$$N = \frac{\frac{\rho q^2}{d} \frac{1}{\epsilon V} \iiint_{(\epsilon V)} \left(-\bar{u}_{rj} \frac{\partial \bar{u}_{ri}}{\partial x_{rj}} - \overline{u'_{rj} \frac{\partial u'_{ri}}{\partial x_{rj}}} \right) (\epsilon\, dV)}{\frac{\mu q}{d^2} \frac{1}{\epsilon V} \iiint_{(\epsilon V)} \frac{\partial^2 \bar{u}_{ri}}{\partial x_{rj} \partial x_{rj}} (\epsilon\, dV)} \tag{41}$$

Equations 40 and 41 are identical and therefore,

$$\frac{\rho q d}{\mu} = \frac{\frac{\rho q^2}{d} \frac{1}{\epsilon V} \iiint_{(\epsilon V)} \left(-\bar{u}_{rj} \frac{\partial \bar{u}_{ri}}{\partial x_{rj}} - \overline{u'_{rj} \frac{\partial u'_{ri}}{\partial x_{rj}}} \right) (\epsilon\, dV)}{\frac{\mu q}{d^2} \frac{1}{\epsilon V} \iiint_{(\epsilon V)} \frac{\partial^2 \bar{u}_{ri}}{\partial x_{rj} \partial x_{rj}} (\epsilon\, dV)}$$

or

$$\frac{1}{\epsilon V}\iiint_{(\epsilon V)} \frac{\partial^2 \bar{u}_{ri}}{\partial x_{rj}\,\partial x_{rj}}\,(\epsilon\, dV) = \frac{1}{\epsilon V}\iiint_{(\epsilon V)}\left(-\bar{u}_{rj}\frac{\partial \bar{u}_{ri}}{\partial x_{rj}} - \overline{u'_{rj}\frac{\partial u'_{ri}}{\partial x_{rj}}}\right)(\epsilon\, dV)$$

or

$$\frac{1}{\epsilon V}\iiint_{(\epsilon V)}\left(-\bar{u}_{rj}\frac{\partial \bar{u}_{ri}}{\partial x_{rj}} - \overline{u'_{rj}\frac{\partial u'_{ri}}{\partial x_{rj}}}\right)(\epsilon\, dV) = \frac{1}{c}\,. \qquad (42)$$

The volumetric integral on the left-hand side of equation 42 is a function of both convective forces and turbulent forces. These forces are a result of two different flow phenomena and cannot, in general, be combined into one constant unless the effects of one of the forces can be neglected.

Writing the equation of pressure gradient in general form, the relative contribution of different terms can be compared. From equation 38 which is

$$\frac{dP}{dx} = \frac{\mu q}{d^2}\frac{1}{\epsilon V}\iiint_{(\epsilon V)} \frac{\partial^2 \bar{u}_{ri}}{\partial x_{rj}\,\partial x_{rj}}\,(\epsilon\, dV) + \frac{\rho q^2}{d}\frac{1}{\epsilon V}\iiint_{(\epsilon V)}\left(-\bar{u}_{rj}\frac{\partial \bar{u}_{ri}}{\partial x_{rj}} - \overline{u'_{rj}\frac{\partial u'_{ri}}{\partial x_{rj}}}\right)(\epsilon\, dV)\;, \qquad (38)$$

it is apparent that pressure gradient is represented by three main factors: shear, convection, and turbulence. It should be borne in mind that energy is dissipated only through viscosity, but the above three factors account for the pressure gradient. For extremely low velocities ($q >> q^2$), the effects of both convection and turbulence are small and can be neglected. Thus, the viscous force

$$\frac{\mu q}{d^2} \; \frac{1}{\epsilon V} \iiint_{(\epsilon V)} \frac{\partial^2 \overline{u}_{ri}}{\partial x_{rj} \, \partial x_{rj}} \quad (\epsilon \, dV)$$

is balanced by the pressure gradient causing the flow. The volume integral in the viscous term has a constant value $\frac{1}{c}$ and represents average geometric effects of the porous medium on the flow. As the flow velocity q is increased, the non-linear effects due to turbulence and convection assume greater importance. For flow through porous media, convective accelerations are always present whereas turbulence is a random phenomena dependent upon time and space geometry.

Schlichting (32) has shown that for flow in a wind tunnel, the maximum turbulence near the wall boundary, with reference to free stream velocity is about six percent; and Liu et al. (25) show that for flow in open channels the maximum turbulence, with reference to free stream velocity, is about 14 percent. Taking the higher figure (14 percent for the turbulence intensity) the convective and turbulent energies per unit volume can be compared as

$$\frac{3 \times \frac{1}{2} \rho u'^2}{\frac{1}{2} \rho \overline{u}^2} = 3(0.14)^2 = 0.0588 \quad .$$

Thus, it is seen that the energy dissipated by turbulence is very small compared to the energy represented by convective terms. As a result, energy losses caused by turbulence for flow through porous media can be safely ignored. Therefore, it may be assumed without appreciable error that

$$\frac{1}{\epsilon V} \iiint\limits_{(\epsilon V)} \left(- \overline{u'_{rj} \frac{\partial u'_{ri}}{\partial x_{rj}}} \right) (\epsilon \, dV) \approx 0 \tag{43}$$

and

$$\frac{1}{\epsilon V} \iiint\limits_{(\epsilon V)} \left(- \bar{u}_{rj} \frac{\partial \bar{u}_{ri}}{\partial x_{rj}} \right) (\epsilon \, dV) = \frac{1}{c}, \tag{44}$$

Substituting the values of the volume integrals in equation 38, the equation of pressure gradient becomes

$$\frac{dP}{dx} = \frac{\mu q}{cd^2} + \frac{\rho q^2}{cd} \tag{45}$$

or

$$\frac{dP}{dx} = \frac{\mu}{k} q + \frac{\rho}{\sqrt{ck}} q^2 \tag{46}$$

which is the equation for space average pressure gradient applicable to linear and non-linear flow through porous media. In terms of the hydraulic gradient, the equation of pressure gradient becomes

$$\phi = \frac{1}{\rho g} \frac{dP}{dx} = \frac{\mu}{\rho g k} q + \frac{1}{g\sqrt{ck}} q^2$$

or

$$\phi = a\,q + bq^2 \tag{47}$$

where

ϕ = Hydraulic gradient

$$a = \frac{\mu}{\rho g k} \tag{48}$$

and

$$b = \frac{1}{g\sqrt{ck}} . \tag{49}$$

Equation 47, relating the hydraulic gradient to the bulk velocity, was developed by analyzing the Navier-Stokes equations in dimensionless form.

Table 1A presents a summary of the equation which describes the relationship of ϕ and q shown in Figure 2. In addition, the standard error of estimate, permeability and particle diameter are also given. The largest value of the standard error of estimate of 6.5% shown in this table is within experimental error. This indicates the quadratic equation obtained from the theoretical analysis describes the data very well. Complete data are tabulated in Appendix D.

The equation of hydraulic gradient can also be written as

$$gcd \frac{\phi}{q^2} = \frac{\mu}{\rho q d} + 1$$

or

$$H = \frac{1}{N} + 1 \tag{50}$$

where

$$H = gcd \frac{\phi}{q^2} \tag{51}$$

TABLE 1A. LIST OF EQUATIONS OBTAINED FOR VARIOUS UNCONSOLIDATED POROUS MEDIA

Investigator	Equation	Medium	S_y %	k (cm^2)	d_s (cm)
N. Ahmed	$\phi = 7.39314q + 0.74532q^2$	Sand	1.5	2.1×10^{-6}	0.054
N. Ahmed	$\phi = 3.80661q + 0.45379q^2$	Sand	1.7	3.96×10^{-6}	0.0764
N. Ahmed	$\phi = 2.299q + 0.30672q^2$	Sand	1.0	6.91×10^{-6}	0.107
N. Ahmed	$\phi = 1.49209q + 0.244832q^2$	Sand	2.5	1.0×10^{-5}	0.1405
N. Ahmed	$\phi = 0.93837q + 0.17931q^2$	Sand	1.0	1.69×10^{-5}	0.1992
N. Ahmed	$\phi = 0.69441q + 0.165050q^2$	Sand	2.0	2.21×10^{-5}	0.258
H. V. Allen	$\phi = 1.47q + 0.142q^2$	Grannular absorbent	3.3	8.6×10^{-6}	0.0855
F. C. Blake	$\phi = 0.149q + 0.0623q^2$	Glass beads	1.6	6.7×10^{-5}	0.32
L. E. Brownell	$\phi = 0.0647q + 0.0183q^2$	Glass beads	1.4	1.5×10^{-4}	0.53
L. E. Brownell	$\phi = 0.08903q + 0.02188q^2$	Nickel saddles	5.0	1.12×10^{-4}	0.334
G. H. Fancher	$\phi = 16.6q + 7.96q^2$	Ottawa sand	4.1	8.2×10^{-7}	0.07
P. H. Forchheimer	$\phi = 0.00408q + 0.0005q^2$	Sand	2.2	2.30×10^{-3}	0.5
P. H. Forchheimer	$\phi = 0.01225q + 0.00092q^2$	Sand	2.1	7.6×10^{-4}	0.3
C. E. Kirkham	$\phi = 0.0089463q + 0.011685q^2$	Marble	4.1	1.197×10^{-3}	1.6
E. Lindquist	$\phi = 0.0674q + 0.0368q^2$	Sand	3.0	1.38×10^{-4}	0.492
E. Lindquist	$\phi = 1.164q + 0.2918q^2$	Sand	4.5	8×10^{-6}	0.105
F. Mobasheri	$\phi = 0.189q + 0.137q^2$	Sand	6.5	4.94×10^{-5}	0.5
D. K. Sunada	$\phi = 0.145q + 0.0648q^2$	Glass spheres	4.4	6.45×10^{-5}	0.3

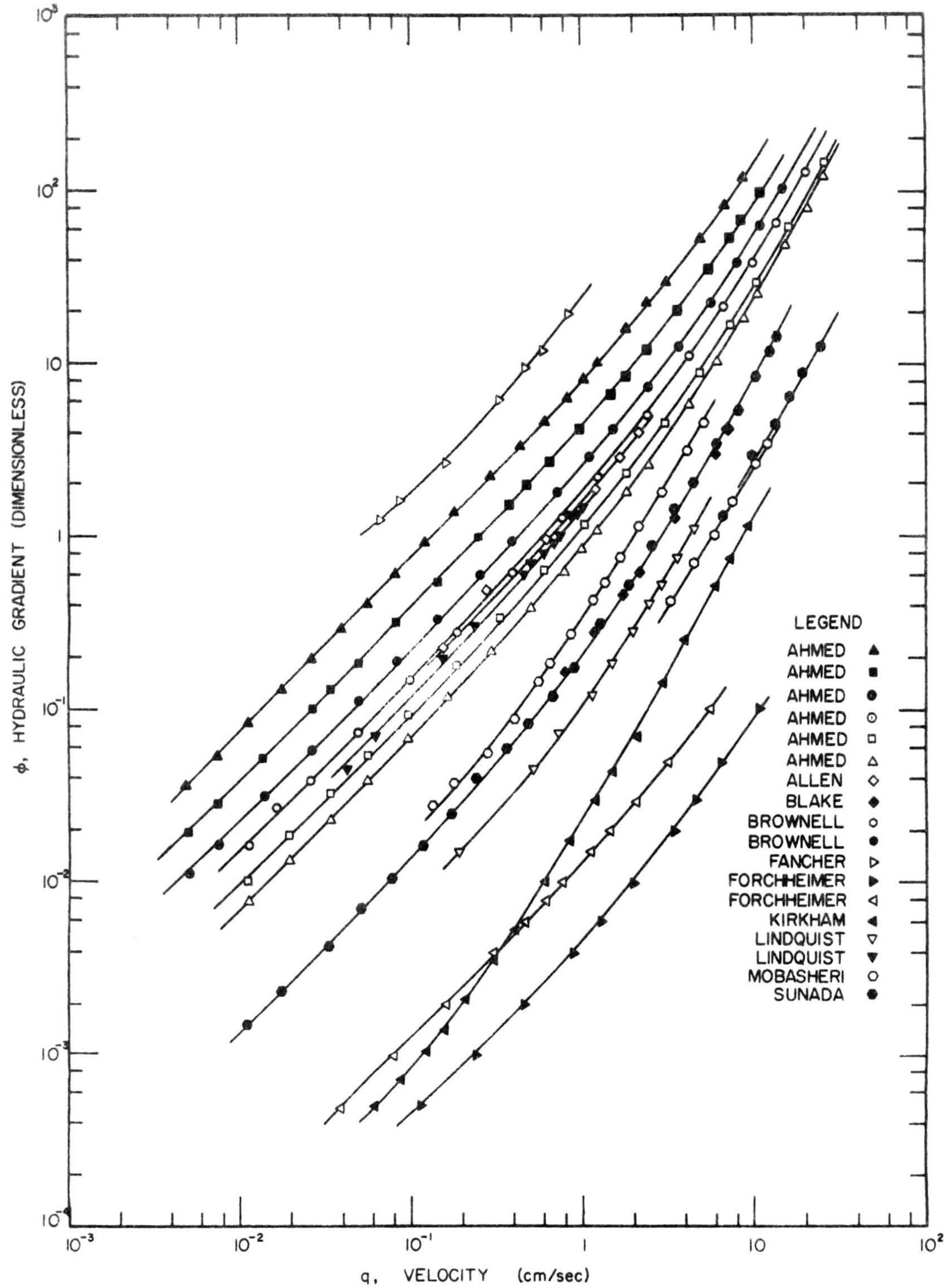

Figure 2. Typical plots of hydraulic gradient versus bulk velocity

and

$$N = \frac{\rho q d}{\mu} \tag{40}$$

A graphical representation of equation 50 should result in a single curve for all porous media in which turbulence may be neglected. The results of 18 tests are presented in Figure 3, which is a plot of H versus N and shows that a single relationship between H versus N exists. Non-linearity becomes predominant at an approximate value of $N = 0.02$. As N becomes large, H approaches unity as predicted by equation 50.

Section 2. Development and Verification of the Physical Characteristics of Porous Media Affecting the Flow Phenomena

Previous investigators have attempted to relate the particle diameter to the characteristic length d without much success. Several investigators used D_{50} which is the average size (50% size) of the particles as obtained from a sieve analysis. However, porous medium, having the same 50% size, will have different pore sizes depending on the distribution of sizes and amount of fine particles present. The configuration and size of the pores depend upon grain size and grain-size distribution. In this section, a statistical analysis of cut-sections for grain size, grain-size distribution, pore size, and pore-size distribution is presented. In addition, relationships between characteristic length d and pore diameter d_p, pore diameter d_p and grain diameter d_g, grain diameter d_g and particle diameter

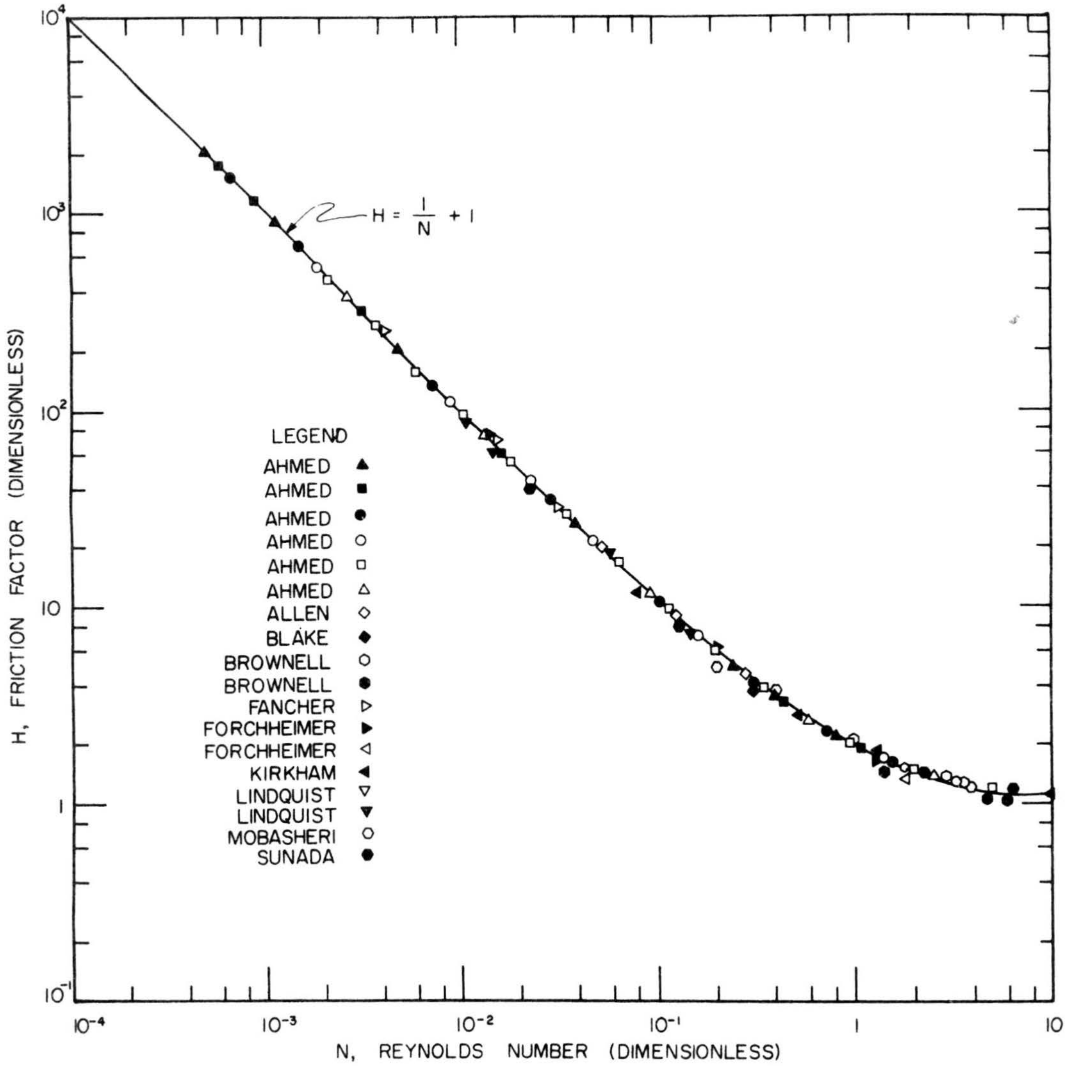

Figure 3. Graphical correlation of friction factor versus Reynolds number

d_s , and characteristic length d and particle diameter d_s are presented. The particle diameter d_s is obtained from sieve analysis whereas the grain diameter d_g is obtained from statistical analysis of cut-section of the porous medium.

There are several methods available for determining grain diameter from cut-section of a porous medium. Krumbein (20) developed a method that describes the frequency distribution of grain diameters obtained from cut-sections providing the grains are spherical in shape and uniform in size. He extended his development to apply to a distribution function for grain populations of variable size. Greenman (15) showed that Krumbein's method is equally applicable to non-spherical grains provided these shapes are approximately ellipsoidal. In making a cut-section analysis, Greenman measured the long diameters of a sufficiently large number of grains and showed satisfactory correlation between loose grain data and cut-section data.

Rosenfeld et al. (29) presented an empirical development for the translation of cut-section distribution to sieve size distribution. They analyzed their data by Greenman's method and gave their concluding remarks that there was no constant relationship between the two techniques which could be recognized.

Packham (27) developed two functions that determine the volume and number frequencies of grain populations of cut-sections and after the application of specific corrections outlined by his method he found excellent correlation between cut-section data and sieve analysis.

Packham's statistical method for determining grain size from cut sections was used for this study. The procedure is presented in Appendix B. Table 1B presents the statistical results of the sieve size, grain size, pore size along with the characteristic length d as obtained by hydraulic measurements for the six porous media used in this study.

TABLE 1B. SOME PHYSICAL PROPERTIES OF THE SIX POROUS MEDIA FOR THE PRESENT INVESTIGATION

Medium	$d_s \times 10$ (cm)	$d_g \times 10$ (cm)	$d_p \times 10$ (cm)	$d \times 10^3$ (cm)
1	0.54	0.54	0.269	1.54
2	0.764	0.762	0.38	1.763
3	1.07	1.075	0.507	2.07
4	1.405	1.4	0.703	2.4
5	1.992	2.0	1.02	2.97
6	2.58	2.58	1.33	3.58

Figure 4 presents a plot of characteristic length d versus pore diameter d_p for the six porous media used in this study. From this figure, the empirical relationship

$$d = 10^{-3} + 2 \times 10^{-2} d_p \tag{52}$$

can be obtained. Equation 52 is valid for d_p in the range between 0.0269 cm to 0.133 cm. The excellent relationship between d and

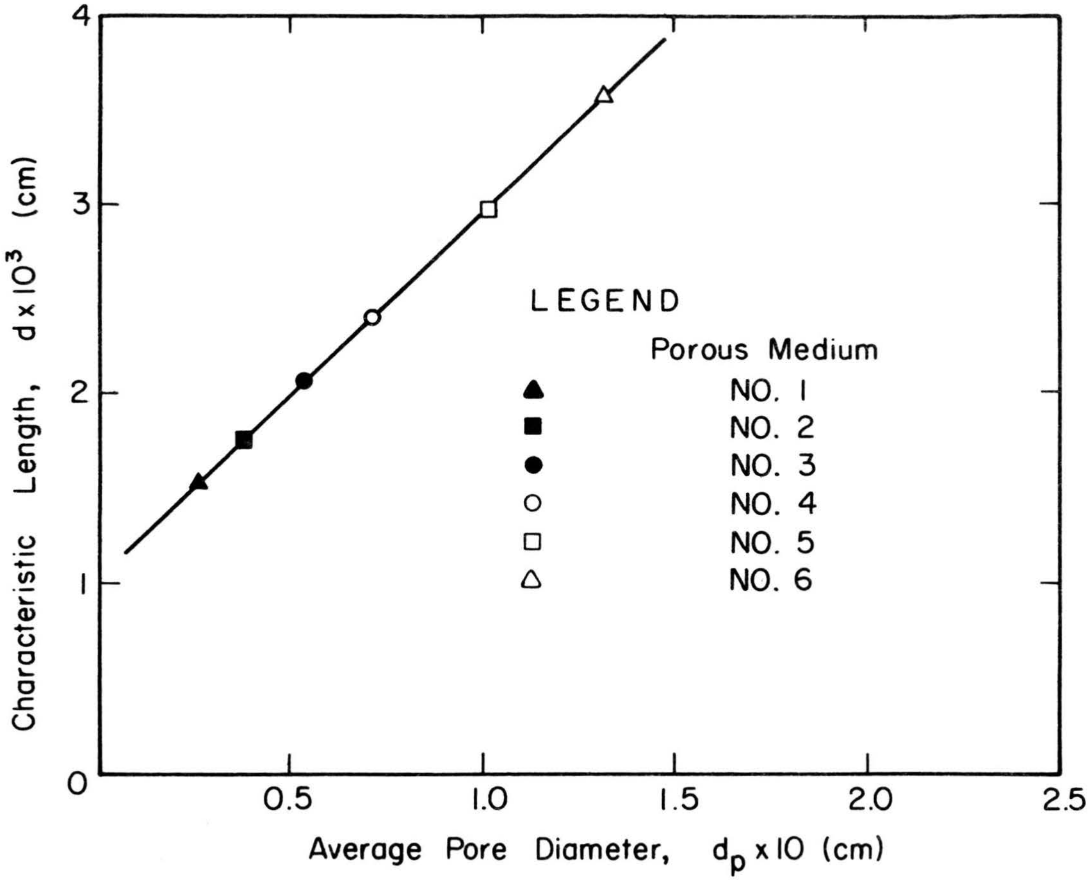

Figure 4. Graphical correlation of characteristic length and average pore diameter

d_p suggests that the characteristic length is dependent upon pore diameter. However, pore diameter is difficult to evaluate whereas particle diameter from sieve analysis is relatively easy to determine. Consequently, a relationship between pore diameter and particle diameter would be desirable.

If one were to drop a long line on a cut-section, then the sum of the length intercepted by the grains plus the sum of the length intercepted by the pores would be equal to the total length and may be expressed as

$$\sum_{i=1}^{n} l_{pi} + \sum_{i=1}^{n} l_{gi} = l_t \tag{53}$$

where l_p would be the length intercepted by the pore, l_g the length intercepted by the grain, and l_t the total length of the line. The average diameter d_p of the pores would be

$$d_p = \frac{\sum_{i=1}^{n} l_{pi}}{N_p} \tag{54}$$

where N_p is the total number of pores intercepted. Likewise, if N_g is the total number of grains intercepted, then,

$$d_g = \frac{\sum_{i=1}^{n} l_{gi}}{N_g} \tag{55}$$

Equation 53 may now be written as

$$d_p N_p + d_g N_g = l_t$$

or

$$d_p = \frac{l_t}{N_p} - \frac{d_g N_g}{N_p}$$

or

$$d_p = c_1 + c_2 d_g \tag{56}$$

where $c_1 = \frac{l_t}{N_p}$ and $c_2 = -\frac{N_g}{N_p}$, and both c_1 and c_2 are constants for a given homogeneous and isotropic media. Equation 56 would be applicable for porous media having about the same shape. In this study, the diameter of the grain from the cut-section was taken as the shorter axis (Appendix B) so that the above analysis would not be strictly valid. However, equation 56 suggests an equation of the form

$$d_p = F(d_g) \quad . \tag{57}$$

Figure 5 shows a plot of d_p versus d_g. From this plot it is evident that

$$d_p = 0.5\, d_g \quad . \tag{58}$$

This relationship is valid only for uniform grain diameter and a different relationship is to be expected for porous medium having a variety of grain sizes.

The relationship between the grain diameter obtained from

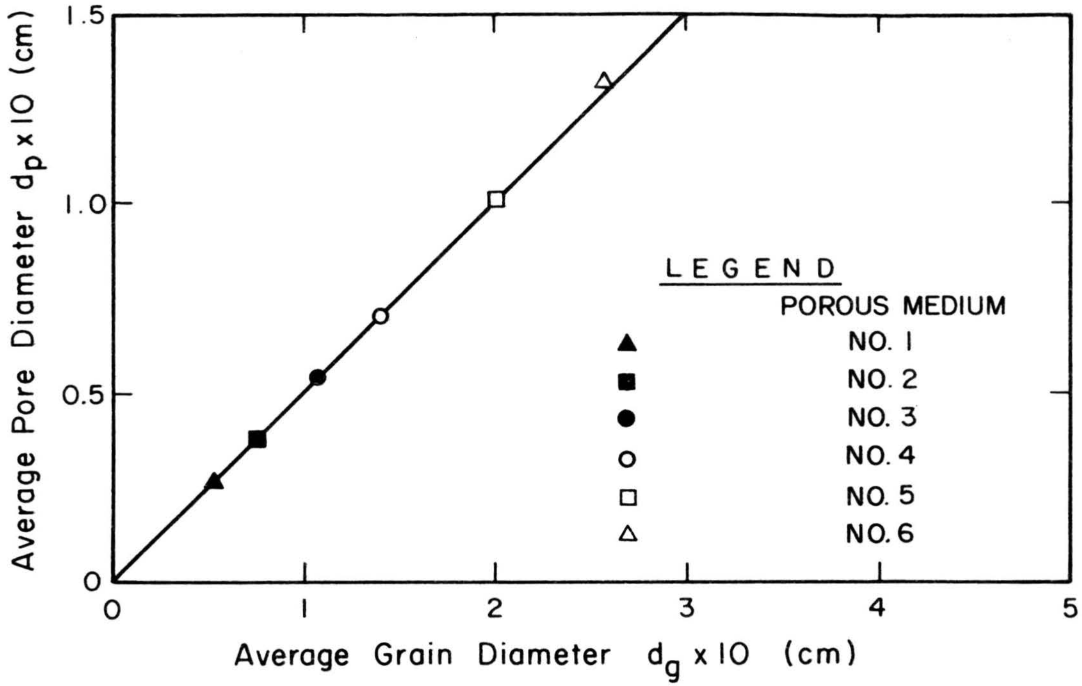

Figure 5. Graphical correlation of average pore diameter and average grain diameter

cut-sections and the particle diameter obtained from sieve analysis is presented in Figure 6. Packham's analysis showed that a one-to-one correspondence should exist between d_g and d_s. Inspection of Figure 6 shows that this is true for grain diameter of uniform size.

From the correlations between d and d_p, d_p and d_g, and d_g and d_s, one would conclude that a correlation between d and d_s would exist. Figure 7 presents this correlation for the six media used in this study and for 12 media studied by other investigators. From this figure the empirical relationship

$$d = 10^{-3} + 10^{-2} d_s \tag{59}$$

can be obtained for d_s larger than 0.054 cm and smaller than 0.258 cm. The spread of points about the line of correlation is explained by the fact that the media used by Brownell, Fancher, Forchheimer and Kirkham were probably not of uniform particle diameter. This indicates that other factors such as pore size distribution must be considered in evaluating the relationship between the characteristic length d and the particle diameter d_s.

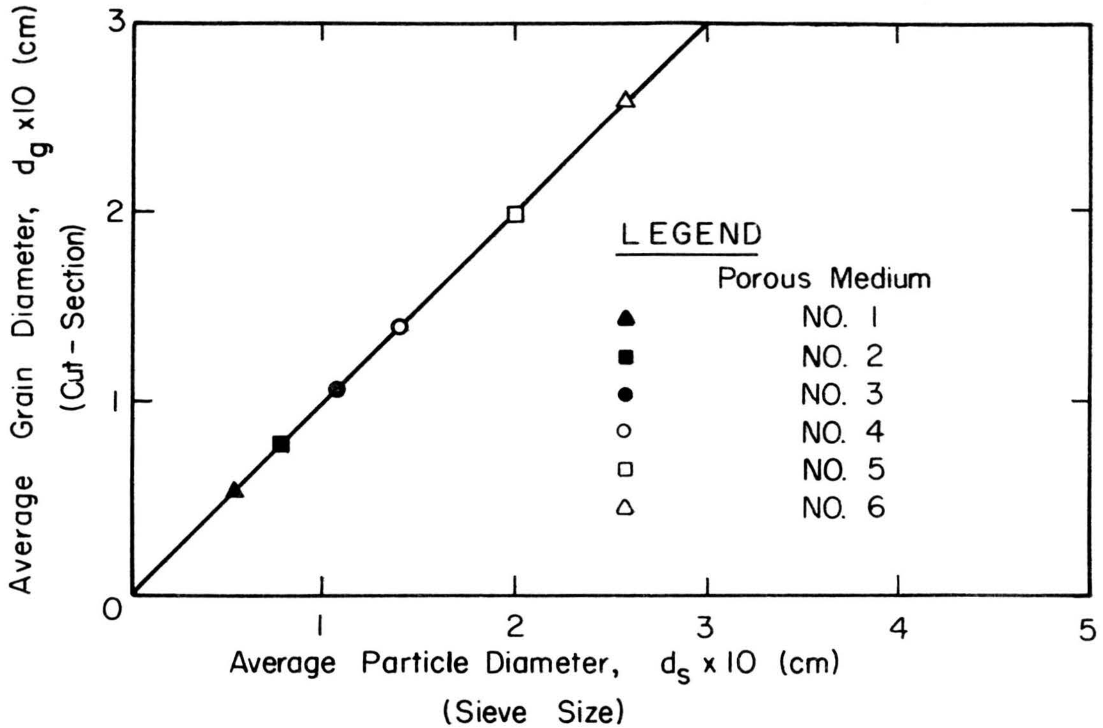

Figure 6. Graphical correlation of average grain diameter and average particle diameter

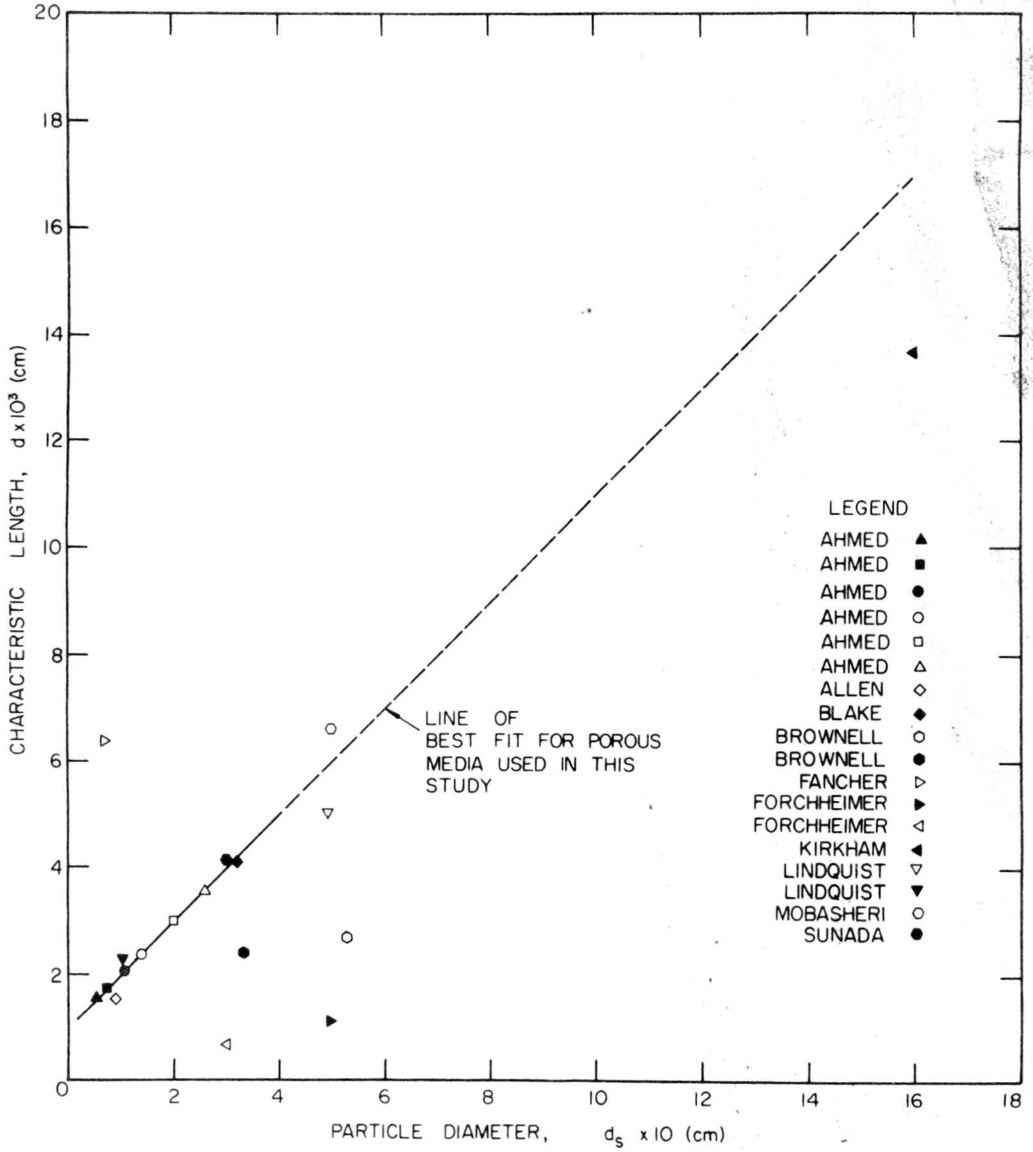

Figure 7. Graphical correlation of characteristic length and particle diameter

Chapter IV

SUMMARY AND CONCLUSIONS

An equation representing the hydraulic gradient as a function of the bulk velocity was developed by analyzing the Navier-Stokes equations in dimensionless form. During the development of the equation it was shown that initial departure from linearity is due to convective accelerations and the effects of turbulence are small and can be neglected.

A unique relationship between friction factor H and Reynolds number N exists for all porous media studied in this investigation. Deviation from Darcy's equation starts at an approximate value of Reynolds number $N = 0.02$.

The characteristic length d, computed from the hydraulic measurments, shows a linear relationship with particle diameter d_s obtained from sieve analysis for uniform grain diameter. It also shows a linear variation with pore diameter d_p and grain diameter d_g obtained from cut-section data of porous media.

The following points need further consideration:

1. To determine the effects upon the flow of variable grain-size distribution.

2. To evaluate the volume integrals,

$$\frac{1}{\epsilon V} \iiint_{(\epsilon V)} \frac{\partial^2 \bar{u}_{ri}}{\partial x_{rj} \partial x_{rj}} \quad (\epsilon \, dV) \quad , \quad \text{and}$$

$$\frac{1}{\epsilon V} \iiint_{(\epsilon V)} \left(- \bar{u}_{rj} \frac{\partial \bar{u}_{ri}}{\partial x_{rj}} - \overline{u'_{rj} \frac{\partial u'_{ri}}{\partial x_{rj}}} \right) (\epsilon \, dV)$$

by geometric probability theories.

3. To refine the electrokinetic probe technique in order to compare the micro-velocities $\bar{u}_i$ and u'_i to substantiate the theoretical development that

$$\frac{1}{2} \rho \bar{u}_i^2 >> \frac{1}{2} \rho u_i'^2 \quad .$$

BIBLIOGRAPHY

BIBLIOGRAPHY

1. Allen, H. V., Pressure drop for flow through beds of granular absorbents. Petroleum Refiner, Vol. 23, No. 7, pp. 247-252, 1944.

2. Blake, F. C., The resistance of packing to fluid flow. Trans. Am. Inst. Chem. Engrs., Vol. 14, pp. 415-421, 1922.

3. Brownell, L. E., and D. L. Katz, Flow of fluids through porous media. Chem. Eng. Prog., Vol. 43, pp. 537-548, 1947.

4. Burke, S. P., and W. B. Plummer, Gas flow through packed columns. Ind. Eng. Chem., Vol. 20, pp. 1196-1200, 1937.

5. Carman, P. C., Fluid flow through grannular beds. Trans. Am. Inst. Chem. Eng., Vol. 15, pp. 150-166, 1937.

6. Corey, A. T., Fluid mechanics of porous solids. Colorado State University, Fort Collins, pp. 30-37, 1965.

7. Cornell, D., and D. L. Katz, Flow of gases through consolidated porous media. Ind. Eng. Chem., Vol. 45, pp. 2145-2152, 1953.

8. Cornfield, J., H. W. Chalkley and R. K. Cook, A problem in geometric probability. Journal of the Washington Acad. of Sciences, Vol. 41, No. 7, pp. 226-229, 1951.

9. Darcy, H. P. G., Les Fontaines publiques de la ville de Dijon, Victor Delmont, Paris, 1856.

10. Ergun, S., Fluid flow through packed columns. Chem. Eng. Prog., Vol. 48, pp. 89-94, 1952.

11. Fair, G. M. and L. P. Hatch, Fundamental factors governing streamline flow of water through sand. Journal Am. Water Works Assoc., Vol. 25, No. 11, pp. 1551-1565, 1933.

12. Fancher, G. H., and J. A. Lewis, Flow of simple fluids through porous materials. Ind. Eng. Chem., Vol. 25, pp. 1139-1147, 1933.

13. Forchheimer, P. H., Wasserbewegun durch boden, Zeitschrift des vereines Deutscher Ingenieure, No. 49, pp. 1736-1749; continued in No. 50, pp. 1781-1788, 1901.

14. Franzini, J. B., Porosity factor for case of laminar flow through granular media. Trans. Am. Geo. Union, Vol. 32, No. 3, pp. 443-446, 1951.

15. Greenman, N. N., The mechanical analysis of sediments from thin-section data. Journal of Geology, Vol. 59, pp. 447-462, 1951.

16. Hubbert, M. K., The theory of ground water motion. Journal of Geology, Vol. 48, pp. 785-944, 1940.

17. Irmay, S., On the theoretical derivation of Darcy and Forchheimer formulas. Trans. Am. Geo. Union, Vol. 39, pp. 702-707, 1958.

18. Kozeny, J., Uber Kapillare Leitung des Wassers im Boden, Sitzber. Akad. Wiss. Wien, Math-naturw. kl., Abt. IIa 136, pp. 271-306, 1927.

19. Kirkham, C. E., Turbulent flow in porous media - An analytical and experimental model study. Doctoral Thesis, University of Melbourne, Melbourne, 1966.

20. Krumbein, W. C., Thin-section mechanical analysis of indurated sediments. Journal of Geology, Vol. 43, pp. 482-496, 1935.

21. Krumbein, W. C., and G. D. Monk, Permeability as a function of the size parameter of unconsolidated sand. Trans. AIME, Vol. 151, pp. 153-163, 1943.

22. Larsen, I., I. C. O'Neill and A. K. Parkin, Turbulent flow in porous media, Discussions, Proc. Am. Soc. Civil Engrs., Journal of the Hydraulics Division, Vol. 91, No. HY2, 1965.

23. Leva, M., M. Weintraub, M. Grummer, M. Pollchik, and H. H. Storch, Fluid flow through packed and fluidized systems. U.S. Bureau of Mines, Bulletin No. 504, 149 pp., 1951.

24. Lindquist, E., On the flow of water through porous soils. 1st Congress des Grands Barrages, Stockholm, Vol. 5, pp. 81-101, 1933.

25. Liu, C. K., S. J. Kline and J. P. Johnston, An experimental study of turbulent boundary layer on rough walls. Department of Mechanical Engineering, Stanford University, Stanford, California. Report MD-15, p. 128, July 1966.

26. Mobasheri, F. and D. K. Todd, Investigation of the hydraulics of flow near recharge wells. Water Resources Centre Contribution No. 72, University of California, Berkeley, 32 pp., 1963.

27. Packham, G. H., Volume, weight and number frequency analysis of sediments from thin-section data. Journal of Geology, Vol. 63, No. 1, pp. 50-58, 1955.

28. Romita, P. L., I limiti di validita della legge di Darcy alla luce dei piu recenti resultati sperimentali. Ricerea Scientifica, Vol. 21, pp. 1978-1998, 1951.

29. Rosenfeld, M. A., L. Jacobson and J. C. Ferm, A comparison of sieve and thin-section technique for size analysis. Journal of Geology, Vol. 61, pp. 114-133, 1953.

30. Rumer, R. R., Longitudinal dispersion in steady and unsteady flow. Proc. Am. Soc. Civil Engrs., Journal of Hydraulics Division, Vol. 88, No. HY4, July 1962.

31. Scheidegger, A. E., The physics of flow through porous media. The Macmillan Co., New York, 1960.

32. Schlichting, H., Boundary layer theory. 4th Ed., McGraw Hill Book Co., pp. 457-472, 1960.

33. Schneebeli, G., Experiences sur la limite de validite de la turbulence dams un ecoulement de filtration. La Houille Blanche, No. 2, pp. 141-149, Mars-Avril, 1955.

34. Sullivan, R. R., Specific surface measurements on compact bundles of parallel fibers. Journal of Applied Physics, Vol. 13, pp. 725-730, 1942.

35. Sunada, D. K., Laminar and turbulent flow of water through homogeneous porous media. Ph. D. Dissertation, University of California, Berkeley, 71 pp., 1965.

36. Sunada, D. K., Turbulent flow in porous media, Discussion, Proc. Am. Soc. Civil Engrs., Journal of the Hydraulics Division, Vol. 90, No. HY5, 1965.

37. Ward, J. C., Turbulent flow in porous media. Proc. Am. Soc. Civil Engrs., Journal of the Hydraulics Division, Vol. 90, No. HY5, pp. 1-12, 1964.

APPENDICES

APPENDIX A

1. EXPERIMENTAL APPARATUS AND MATERIALS

The flow diagram of the experimental apparatus used in this study is shown in Figure 8. A brief description of apparatus and materials used is given here.

Permeameter

The permeameter was constructed of plexiglass tubing with wall thickness of 0.635 cm, and inside nominal diameter of 6.35 cm. Four pressure taps were fixed 12.7 cm apart from one another, and the overall length of the permeameter was about 68 cm. The permeameter was provided with top and bottom flanges to be coupled with inlet and outlet supply pipes. The top and bottom of the permeameter was fitted with a perforated steel plate that could be fixed in place after packing the medium. The steel plate at the top was designed to hold the medium in place throughout the entire testing period. After the hydraulic tests were completed, the permeameter could then be removed from the connecting pipes without rearrangement of the particles in the medium. Figure 9 shows the general features of construction of the permeameter.

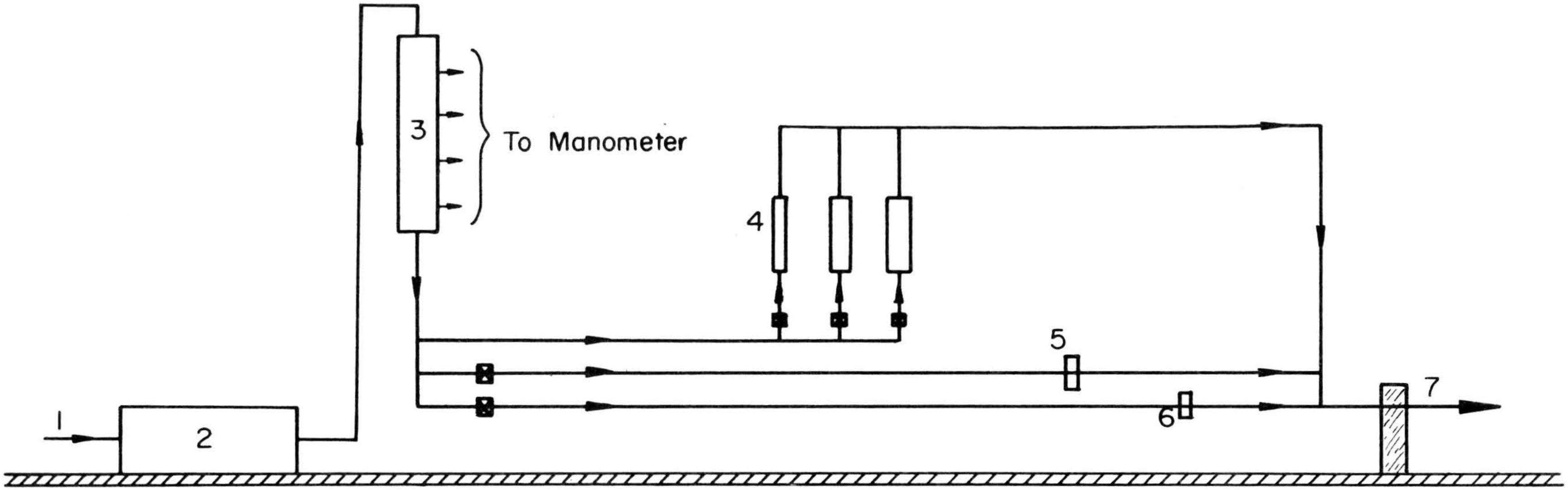

1 Supply Line
2 Centrifugal Pump
3 Permeameter
4 Flowmeters
5 Small Orifice Meter
6 Large Orifice Meter
7 Sump Line

Figure 8. Flow diagram of experimental equipment used for study

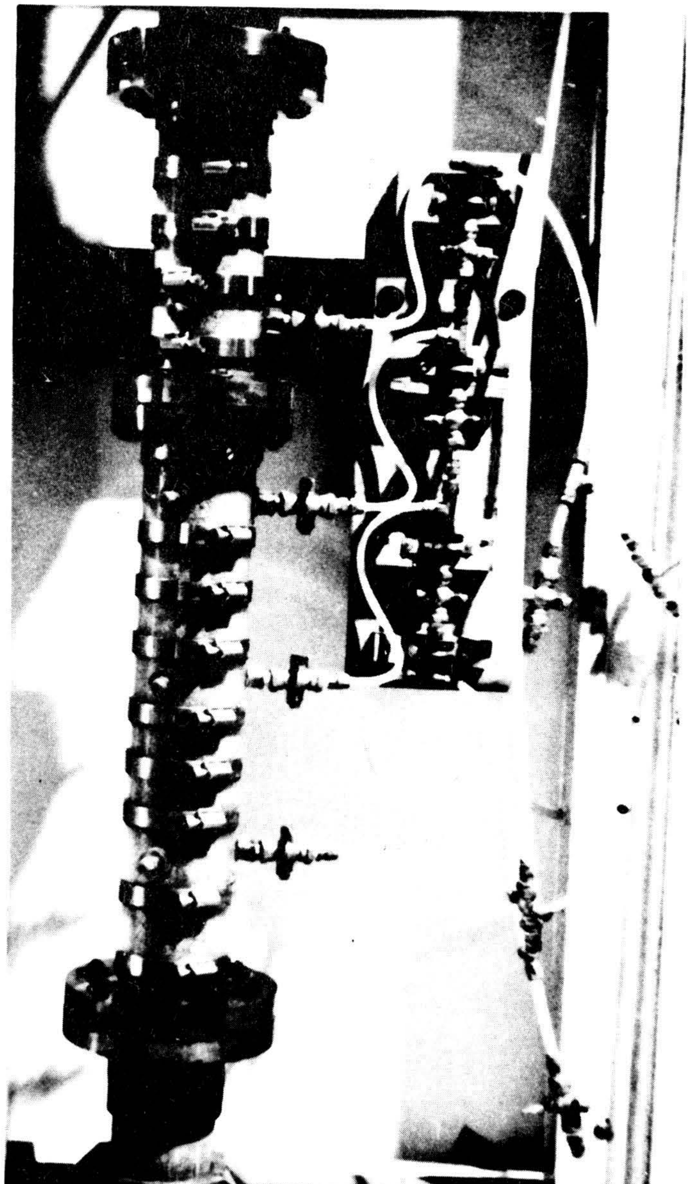

Figure 9. Permeameter shown with four pressure taps, top and bottom flanges, and reinforcing clamps

Flowmeters

Three flowmeters of Fischer & Porter Co., Hatboro, Pennsylvania, were fixed on the discharge end of the permeameter to measure the flow rate. Their measurement accuracy was checked before the start of the experiment. The range of the smallest flowmeter was from 0 to 3.3 cc/sec., the medium sized from 3.0 cc/sec. to 37.8 cc/sec. and the largest one from 33 cc/sec. to 410 cc/sec.

Orifice Meters

Two orifice meters of sizes 2.54 cm and 5.08 cm were installed in conjunction with the flowmeters to measure higher flow rates. They were calibrated before the start of the experiment. Flow rates as high as 7000 cc/sec. could be measured.

Water Supply

Water was obtained directly from Horsetooth Reservoir at a static pressure of about 75 psi. A centrifugal pump was used to develop a total of 120 psi pressure at a flow rate of about 200,000 cc/sec.

Material

Poudre River sand was used as porous medium. Sand was obtained from the Sterling Sand & Gravel Co., Fort Collins, Colorado. Table 2 shows the sieve separates used for the six porous media.

TABLE 2

SIEVE SEPARATES FOR SIX POROUS MEDIA FOR THE PRESENT INVESTIGATION

Porous Medium	Sieve # (Tyler Series)	Sieve Size (cm)	d_s (cm)
1	28	0.0595	0.054
	32	0.0489	
2	20	0.0833	0.0764
	24	0.0701	
3	14	0.1168	0.107
	16	0.0991	
4	10	0.168	0.1405
	14	0.1168	
5	8	0.2362	0.1992
	10	0.168	
6	7	0.283	0.258
	8	0.2362	

2. EXPERIMENTAL PROCEDURE AND EVALUATION OF DATA

The procedure followed in the experimental study and evaluation of data is briefly outlined as follows.

Preparation of Sample

Each sand sample consisted of size separates as shown in Table 2. The sample was thoroughly washed and packed into the permeameter in layers of about 2 cm thickness. The pressure difference between adjacent taps was measured for a given flow rate. If the overall error of pressure difference was within 5% , the sample was accepted as being homogeneous. Otherwise, packing was repeated until the error was within 5%.

Hydraulic Measurements

The measurements consisted of measuring the pressure drop across two pressure taps, discharge measurement, and the temperature of the liquid. The temperature was measured throughout the run and it was found that it remained essentially constant. For larger pressure differences, the mercury manometer was used and for smaller pressure differences the water manometer was used.

Porous Media Sample for Cut-Sections

After the hydraulic measurements were completed, the permeameter was removed without disturbing the medium. The porous medium was then dried by passing air through the permeameter. Epoxy resin was then poured in the middle of the section of permeameter from the top and was allowed to set. The consolidated porous medium was then taken out, put into another small cardboard cylinder, and saturated with more epoxy resin. At least twenty-four hours setting time was given to each sample before cutting with a diamond saw. Slides of the cut-sections were then taken for statistical analysis. A photograph of the cut-section of porous medium No. 2 is shown in Figure 10.

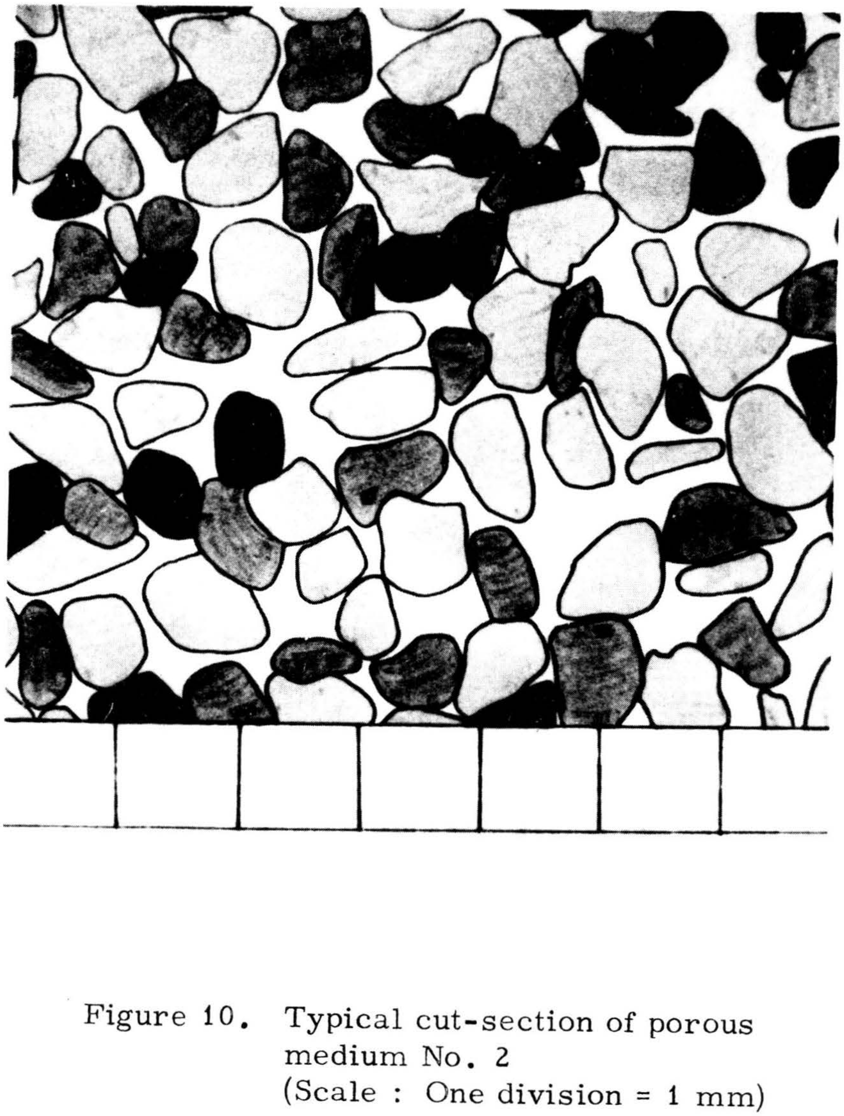

Figure 10. Typical cut-section of porous medium No. 2
(Scale : One division = 1 mm)

Reduction of Data

The constants a and b were computed by the following formulas given by Sunada (38):

$$a = \frac{\sum_{i=1}^{n} \phi_i/q_i \sum_{i=1}^{n} q_i^2 - \sum_{i=1}^{n} q_i \sum_{i=1}^{n} \phi_i}{n \sum_{i=1}^{n} q_i^2 - \left(\sum_{i=1}^{n} q_i\right)^2} \tag{60}$$

$$b = \frac{n \sum_{i=1}^{n} \phi_i - \sum_{i=1}^{n} \phi_i/q_i \sum_{i=1}^{n} q_i}{n \sum_{i=1}^{n} q_i^2 - \left(\sum_{i=1}^{n} q_i\right)^2} \tag{61}$$

After the computation of a and b , the percent standard error of estimates S_y was calculated as

$$S_y = \left[\frac{\sum_{i=1}^{n} \left(\frac{\phi_i - aq_i - bq_i^2}{\phi_i} \right)^2}{n} \right]^{\frac{1}{2}} \tag{62}$$

The values of k , c , and d were computed from the following equations:

$$k = \frac{\mu}{a\rho g} \tag{46}$$

$$c = \frac{1}{b^2 \rho g k} \tag{47}$$

$$d = \sqrt{\frac{k}{c}} \tag{1}$$

APPENDIX B

STATISTICAL ANALYSIS

The procedure followed for statistical analysis of cut-sections is briefly outlined in this appendix. Section 1 describes the method for determining the average grain diameter from cut-sections of porous media embedded in the epoxy, and Section 2 describes the procedure for evaluating porosity, specific surface area, and the average pore diameter.

Section 1

Average Grain Diameter

Several color slides were prepared from cut-sections of all the porous media. The slides were projected on paper and outlines of grain cross-sections were traced. An arbitrary coordinate axes system was rotated around the grain cross-section until two perpendicular dimensions, one being the minimum of all the grain dimensions, were obtained. The minimum length dimension of the grain cross-section was termed the shorter axis and was recorded in its respective class-interval. Figure 11 shows the procedure for measuring the shorter axis of the grain cross-sections. Table 3 shows the percent

TABLE 3. FREQUENCY DISTRIBUTION OF GRAIN SIZE OF CUT-SECTIONS OF POROUS MEDIUM NO. 5

Magnification = 16x

Class Interval (mm)	Cut-Section Grain Diameter d_i (mm)	% Frequency
4.5 - 9.5	0	0
9.5 - 14.5	12	3.0
14.5 - 19.5	17	9.4
19.5 - 24.5	22	23.6
24.5 - 29.5	27	31.6
29.5 - 34.5	32	18.4
34.5 - 39.5	37	8.8
39.5 - 44.5	42	5.2
44.5 - 49.5	47	0

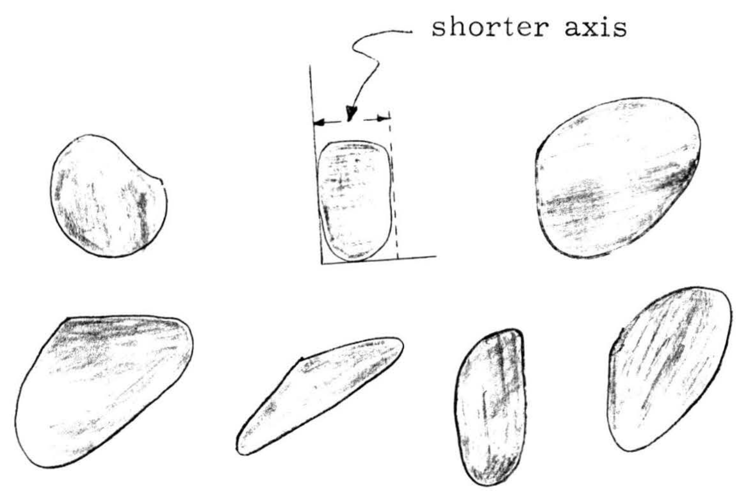

Figure 11. Measurement of shorter axis of grain sections of a cut-section

frequency distribution for porous medium No. 5 with sieve diameter (d_s) of grains of 0.1992 cm.

Table 4 shows how the correction of Packham's method can be applied to the cut-section data. A cumulative percent frequency curve is drawn on semi-log paper, the grain diameter being plotted on the log scale. Values of cumulated percentage frequency, from the largest size down to twice the size for each grain size under consideration, were read off the curve (Figure 12). Also, the percentages between the ranges 2 to 1.5, 1.5 to 1.25, 1.25 to 1.1, and 1.1 to 1.0 times the size under consideration, were read off the curve. Each of these values was multiplied with the appropriate constant given in respective columns of Table 4. The values of these constants have been taken from the original paper of Packham. The products thus obtained were added to get the true distribution for each size.

Table 5 shows the average grain diameter and standard deviation that was obtained by taking first and second moments of each frequency distribution about the center of gravity of the total frequency distribution. The actual diameter and standard deviation were obtained by dividing the respective values of the two quantities by the magnification magnitude. A cut-section containing about one hundred grains was found satisfactory for the purpose of analysis.

TABLE 4. APPLICATION OF CORRECTION OF PACKHAM'S METHOD TO UNCORRECTED CUT-SECTION DATA

d_i (mm)	Cummulative % Frequency	Cummulative % from the largest size to twice the size under consideration; constant = 1.000	Percentage between 2 to 1.5 times the size under consideration; constant = 1.060	Percentage between 1.5 to 1.25 times the size under consideration; constant = 1.164	Percentage between 1.25 to 1.1 times the size under consideration; constant = 1.407	Percentage between 1.1 to 1.0 times the size under consideration; constant = 3.009	Reconstructed cummulative % frequency
12	100	-	-	-	-	-	100
17	97.0	23.8	51.9	20.5	7.3	6.6	100
22	87.6	3.5	24.8	39.6	25.3	25.9	100
27	64.0	0.0	7.4	19.8	34.6	46.3	100
32	32.4	0.0	1.6	7.3	15.5	40.9	65.3
37	14.0	0.0	0.0	2.4	6.3	22.3	31.0
42	5.2	0.0	0.0	0.0	3.0	9.3	12.3
47	0.0	0.0	0.0	0.0	0.1	5.4	5.5

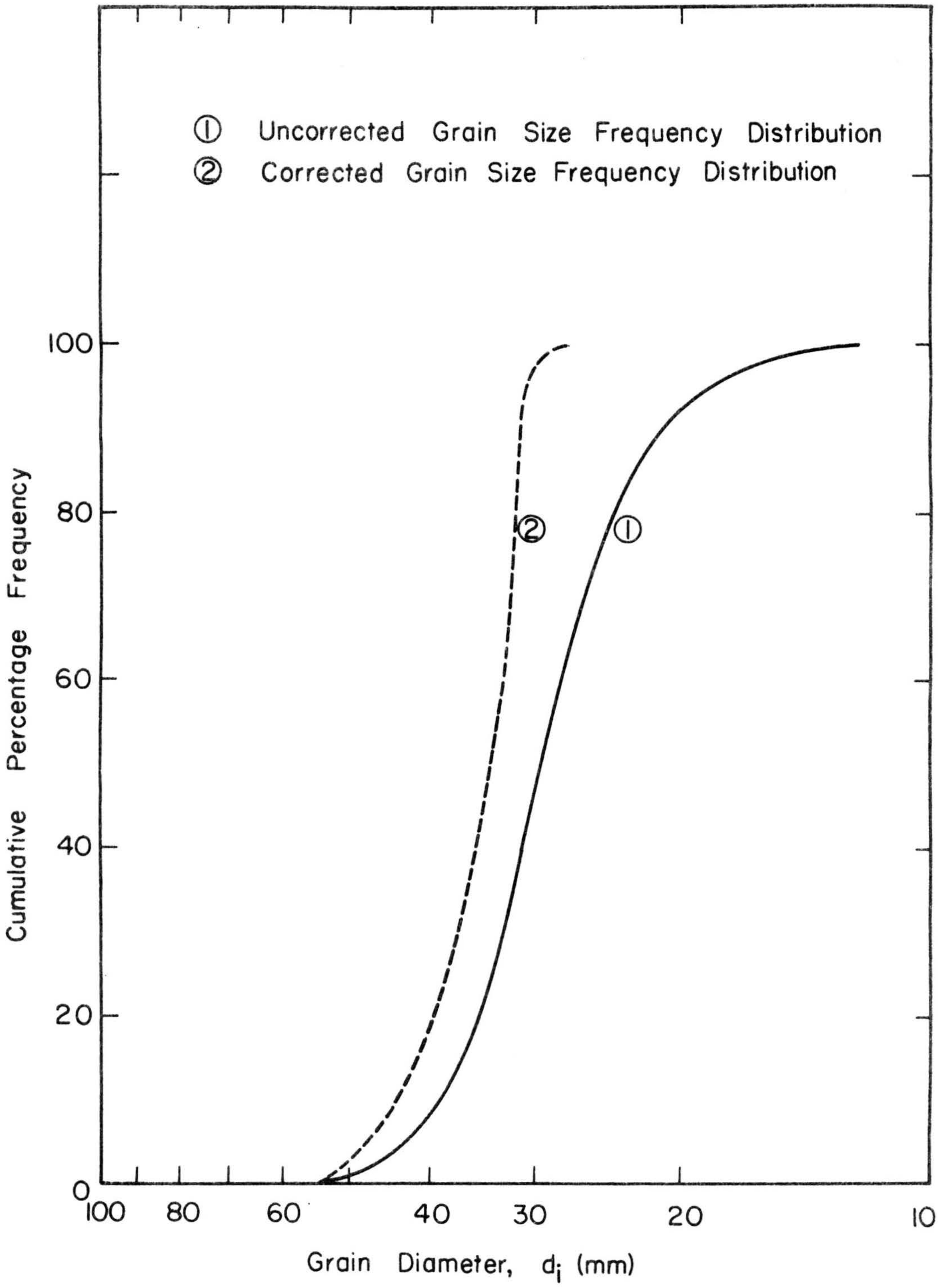

Figure 12. Graphical representation of uncorrected and corrected grain size frequency distributions

TABLE 5. DETERMINATION OF AVERAGE GRAIN DIAMETER OF CUT-SECTION OF POROUS MEDIUM NO. 5

d_i (mm)	f %	f d_i (mm)	$d_i - \bar{\mu}$ (mm)	$(d_i - \bar{\mu})^2$ (mm)^2	f $(d_i - \bar{\mu})^2$ (mm)^2
27	34.7	936.9	-5.7	32.5	1127.8
32	34.3	1097.6	-0.7	0.5	17.7
37	18.7	691.9	4.3	18.5	346.0
42	6.8	285.6	9.3	86.5	588.2
47	5.5	258.5	14.3	204.5	1124.8
$\sum$	100	3270.5			3204.5

Average diameter $\bar{\mu}$ = 32.705 mm

Standard deviation $\sigma_g = \pm\sqrt{\frac{3204.5}{99}} = \pm\ 5.7$ mm

Actual average diameter of grains = $d_g = \frac{\bar{\mu}}{\text{Magnification}}$

$$= \frac{32.705}{16} \approx 2 \text{ mm}$$

Actual standard deviation = $\pm\ 0.356$ mm

Section 2

a. Specific Surface and Porosity

To find the specific surface and porosity of any porous medium, a needle with a length of about twice the size of the average grain diameter was dropped at random on the cut-sections, The data for porous medium No. 5 was recorded in Table 6.

TABLE 6. DETERMINATION OF SPECIFIC SURFACE AND POROSITY

No. of Throws	No. of Cuts	No. of Hits	No. of Misses	S_V (cm^{-1})	ϵ_c %
51	236	61	41	33.9	40.2

A cut is defined when the needle crosses the boundary of a grain cross-section. If one or both ends of the needle fall within a grain cross-section, one or two hits are registered respectively. Similarly, misses would be recorded when the needle ends are found in the pore space. Figure 13 shows the way to determine the above mentioned terms. About fifty throws were found adequate to get satisfactory results. The specific surface and the porosity were found by equations 63 and 64 respectively.

$$S_V = \frac{4\ E(c)\ M}{l_n\ E(h)} \tag{63}$$

and

$$\epsilon_c = \frac{E\,(p)}{E\,(t)} \tag{64}$$

where

S_v = Specific surface of grains

$E\,(c)$ = Expected number of cuts

$E\,(h)$ = Expected number of hits

l_n = Length of the needle

ϵ_c = Porosity of a cut-section

$E\,(p)$ = Expected hits in pores

$E\,(t)$ = Total hits in pores and grain sections

M = Magnification.

Specific surface and porosity have been determined for the sake of completion of basic data.

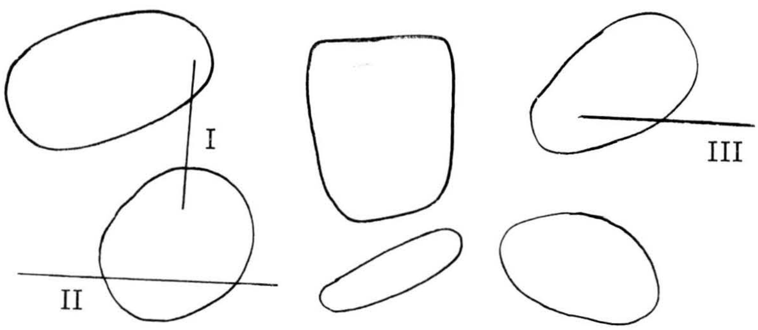

Figure 13. Measurement of specific surface and porosity

[Throw # I, 2 cuts and 2 hits

Throw # II, 2 cuts and 2 misses

Throw # III, 1 cut, 1 hit and 1 miss]

b. Average Pore Diameter

Lines were dropped at random on the cut-sections and pore lengths were recorded as shown in Figure 14. Frequency distribution of pore lengths with arbitrary class intervals was computed and was recorded in Table 7. The average pore diameter and standard deviation were computed by taking first and second moments of individual frequency distributions about the center of gravity of total frequency distribution. Values of pore diameter and standard deviation thus obtained were divided by the magnification of the cut-section to get the actual pore diameter and standard deviation. About one hundred pore lengths were found adequate to get satisfactory results.

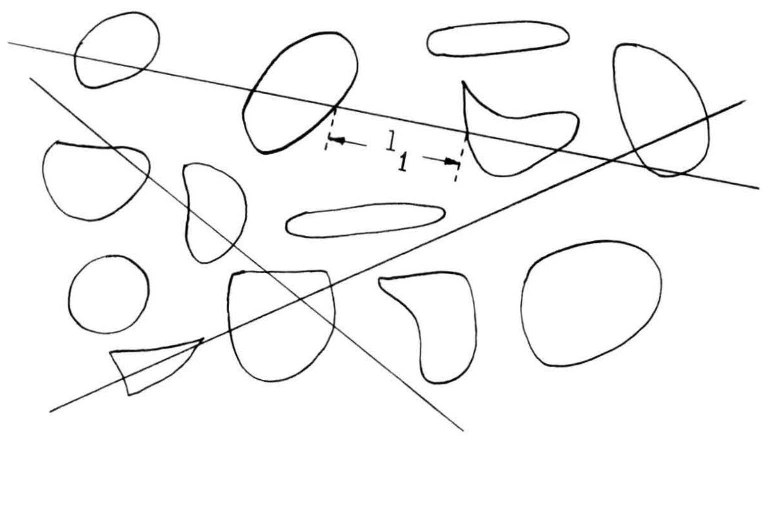

Figure 14. Typical random lines and pore lengths (l_1, ...) of a cut-section

TABLE 7. DETERMINATION OF AVERAGE PORE DIAMETER

d_{pi} (mm)	f %	$f\ d_{pi}$ (mm)	$d_{pi} - \bar{\mu}_p$ (mm)	$(d_{pi} - \bar{\mu}_p)^2$ $(mm)^2$	$f\ (d_{pi} - \bar{\mu}_p)^2$ $(mm)^2$
2	11.9	23.8	-14.3	204.5	2433.6
7	15.2	106.4	- 9.3	86.5	1314.8
12	17.9	214.8	- 4.3	18.5	331.2
17	24.5	416.5	0.7	0.5	12.2
22	11.3	248.6	5.7	32.5	367.3
27	7.9	213.3	10.7	114.5	904.6
32	5.3	169.6	15.7	246.5	1306.5
37	3.3	122.1	20.7	428.5	1414.1
42	2.0	84.0	25.7	660.5	1321.0
47	0.7	32.9	30.7	942.5	659.8
Σ	100	1632.0			10065.1

[Magnification 16x]

Average pore diameter $= \dfrac{1632}{100} = 16.32$ mm

Standard deviation $= \sqrt{\dfrac{10065.1}{99}} = \pm\ 10.09$ mm

Actual average pore diameter $= d_p = \dfrac{16.32}{16} = 1.02$ mm

Standard deviation $= \sigma_p = \pm\ 0.63$ mm

APPENDIX C

LIST OF SYMBOLS

Symbols along with their description and units are given here:

Symbol	Description	Units
A	Available cross-sectional area	L^2
A_g	Surface area of grains	L^2
A_t	Total cross-sectional area	L^2
a	Constant	T/L
a'	Constant	FT/L^4
B	Length parameter characterizing the size of a tube	L
b	Constant	T^2/L^2
b'	Constant	FT^2/L^5
c	Constant	- -
c_1, c_2	Constants	- -
D	Average or effective diameter of particles	L
D_{50}	50% grain size of porous media	L
D_p	Effective diameter of pore structure	L
d	Characteristic length of flow	L
d_g	Average grain diameter from a cut-section	L
d_i	Cut-section grain diameter under consideration	L

LIST OF SYMBOLS - Cont'd.

Symbol	Description	Units
d_p	Average pore diameter from a cut-section	L
d_{pi}	Pore diameter under consideration	L
d_s	Particle diameter from sieve analysis	L
E(c)	Expected number of cuts	- -
E(h)	Expected hits in grain sections	- -
E(p)	Expected hits in pore area	- -
E(t)	Expected total hits	- -
e	Thickness of flow over a flat plate	L
F	Function of	- -
f	Frequency	- -
f_ϵ	Friction factor dependent upon porosity	- -
f_v	Ratio of pressure to viscous forces	- -
G	Mass rate of flow	FT/L^3
g	Acceleration of gravity	L/T^2
H	Friction factor dependent upon d	- -
$\vec{I}_1, \vec{I}_2, \vec{I}_3$	Unit vectors in x, y, and z directions, respectively	$L\theta$
i	Component, and i = 1, 2, 3	- -
j	Repeated operator, and j = 1, 2, 3	- -
K	Darcy's coefficient of permeability	L/T
k	Permeability	L^2

LIST OF SYMBOLS - Cont'd.

Symbol	Description	Units
l	Length of porous medium sample	L
l_e	Tortuous length	L
l_g	Length intercepted by a grain	L
l_n	Length of a needle	L
l_p	Length intercepted by a pore	L
l_t	Length of a random line	L
M	Magnification	- -
m	Molecular weight of a gas	- -
m_1	Exponent	- -
N	Reynolds number dependent upon d	- -
N_g	Number of grains intercepted by a random line	- -
N_p	Number of pores intercepted by a random line	- -
n	Number of observations	- -
n_1	Exponent	- -
$\vec{n}$	Unit normal vector to a surface	$L\theta$
P	Space average pressure at a point	F/L^2
p	Pressure at a point	F/L^2
$\bar{p}$	Time average pressure at a point	F/L^2
p'	Fluctuations of pressure about the average pressure at a point	F/L^2

LIST OF SYMBOLS - Cont'd.

Symbol	Description	Units
q	Darcy's velocity or bulk velocity	L/T
R	Gas constant	$L^2/T^2\theta$
R_D	Reynolds number dependent upon D	- -
R_ϵ	Reynolds number dependent upon ϵ	- -
r	Ratio subscript denoting dimensionless variable	- -
r_p	Radius of a particle	L
r_t	Radius of a tube	L
S_1, S_2, S_3	Surfaces in a porous system	L^2
S_v	Specific surface	L^{-1}
S_y	% estimate of standard error	- -
T_o	Tortuosity	- -
T_1	Absolute temperature	θ
u_i	Microscopic velocity in the i-th direction	L/T
$\overline{u}_i$	Time average microscopic velocity in the i-th direction	L/T
u'_i	Fluctuations in velocity about the mean velocity at a point in the i-th direction	L/T
V	Bulk volume of a porous medium	L^3
V_g	Volume of grains in a porous medium	L^3
$\overline{V}$	Average velocity in a cross-section	L/T
z_1	Compressibility factor of a gas	- -

LIST OF SYMBOLS - Cont'd.

Symbol	Description	Units
α	Numerical shape factor	- -
β	Numerical shape factor	- -
ϵ	Porosity (measured)	- -
ϵ_c	Porosity from cut-sections	- -
ζ	Shape factor	- -
ζ_1	Shape factor dependent upon pore structure	- -
ζ_2	Correction factor	- -
θ_o	Angle	- -
μ	Dynamic viscosity	FT/L^2
$\overline{\mu}$	Average diameter of grains from a cut section	L
$\overline{\mu}_p$	Average diameter of pores from a cut section	L
ξ	A ratio length parameter	L
ρ	Density	FT^2/L^4
σ_g	Standard deviation of grain size distribution of a cut-section	L
σ_p	Standard deviation of pore size distribution of a cut-section	L
ϕ	Hydraulic gradient	- -

APPENDIX D

SUMMARY OF DATA

TABLE 8

Investigator: N. Ahmed

Properties of Media: Sand; $d_s = 0.054$ cm; $k = 2.10 \times 10^{-6}$ cm^2
$\epsilon = 41.3\%$; $\epsilon_c = 40.7\%$; $d_g = 0.054$ cm; $d_p =$
0.0269 cm; $S_v = 130.0$ cm^{-1}

Properties of Fluid: $\mu = 0.01524146 \dfrac{\text{dyne-sec}}{\text{cm}^2}$; $\rho = 1.0 \dfrac{\text{gm}^*}{\text{cm}^3}$

Equation: $\phi = 7.39314\,q + 0.74532\,q^2$;

$S_y = 1.5\%$; $c = 0.89$

$d = 1.54 \times 10^{-3}$ cm

Equation valid for the range of velocities from 0.00489 cm/sec to

8.70 cm/sec

ϕ unitless	q cm/sec	H unitless	$N \times 10^4$ unitless
0.0362	0.00489	2036	4.941
0.0543	0.00733	1359	7.406
0.0827	0.0112	889	11.32
0.1016	0.0137	726	13.84
0.131	0.0176	568	17.78
0.146	0.0196	493	19.80
0.196	0.0264	378	26.67
0.254	0.0342	292	34.56
0.298	0.0401	249	40.52

* gm = gram

TABLE 8 - Cont'd.

ϕ unitless	q cm/sec	H unitless	N x 10^4 unitless
0.364	0.0489	204.6	49.41
0.418	0.0562	177.9	56.78
0.509	0.0684	146.2	69.11
0.617	0.0826	121.5	83.46
0.727	0.0973	103.2	98.31
0.823	0.110	91.41	111.1
0.906	0.121	83.18	122.3
1.073	0.143	70.50	144.5
1.249	0.166	60.94	167.7
1.394	0.185	54.75	186.9
1.680	0.222	45.81	224.3
1.920	0.253	40.32	255.6
2.255	0.296	34.59	299.1
2.578	0.337	30.51	340.5
2.983	0.388	26.63	392.0
3.424	0.443	23.45	447.6
3.878	0.499	20.92	504.2
4.328	0.554	18.95	559.8
4.791	0.610	17.31	616.3
5.250	0.665	15.95	671.9
5.722	0.721	14.80	728.5
6.191	0.776	13.82	784.1
6.671	0.832	12.95	840.7
7.150	0.887	12.21	896.2
7.631	0.942	11.56	951.8
8.128	0.998	10.97	1008
8.591	1.05	10.47	1061
9.132	1.11	9.96	1122
10.415	1.25	8.96	1263
12.971	1.52	7.54	1536
16.24	1.85	6.38	1869
22.72	2.46	5.04	2486
30.11	3.10	4.21	3132
37.60	3.70	3.69	3738
45.90	4.32	3.30	4365
53.79	4.94	2.96	4991
64.53	5.58	2.78	5638
74.57	6.20	2.61	6264

TABLE 8 - Cont'd.

ϕ unitless	q cm/sec	H unitless	N x 10^4 unitless
84.66	6.79	2.47	6861
96.19	7.43	2.34	7507
107.94	8.05	2.24	8134
120.88	8.70	2.15	8790

TABLE 9

Investigator: N. Ahmed

Properties of Media: Sand; $d_s = 0.0764$ cm; $k = 3.96 \times 10^{-6}$ cm^2;

$\epsilon = 41.4\%$; $\epsilon_c = 40.5\%$; $d_g = 0.0762$ cm ;

$d_p = 0.038$ cm; $S_v = 92.5$ cm^{-1} .

Properties of Fluid: $\mu = 0.01480482 \dfrac{\text{dyne-sec}}{\text{cm}^2}$; $\rho = 1.0 \dfrac{\text{gm}}{\text{cm}^3}$

Equation: $\phi = 3.80661\, q + 0.45379\, q^2$; $S_y = 1.7\%$; $c = 1.274$;

$d = 1.763 \times 10^{-3}$ cm.

Equation valid for the range of velocities from 0.00489 cm/sec to 11.14 cm/sec.

ϕ unitless	q cm/sec	H unitless	$N \times 10^4$ unitless
0.0189	0.00489	1742	5.82
0.0283	0.00733	1161	8.73
0.0425	0.0112	749	13.34
0.0528	0.0137	619	16.31
0.0669	0.0176	475.6	20.96
0.0748	0.0196	429.3	23.34
0.1008	0.0264	318.7	31.44
0.131	0.0342	246.8	40.73
0.154	0.0401	211.1	47.75
0.187	0.0489	172.3	58.23
0.216	0.0562	150.7	66.92
0.261	0.0684	122.9	81.45
0.318	0.0826	102.7	98.36
0.376	0.0973	87.5	115.87
0.425	0.110	77.6	131.0
0.468	0.121	70.46	144.1
0.554	0.143	59.70	170.3
0.646	0.166	51.66	197.7
0.721	0.185	46.43	220.3
0.869	0.222	38.85	264.4
0.994	0.253	34.23	301.3

TABLE 9 - Cont'd.

ϕ unitless	q cm/sec	H unitless	N x 10^4 unitless
1.169	0.296	29.40	352.5
1.34	0.337	26.01	401.3
1.55	0.388	24.15	462.0
1.78	0.443	19.99	527.5
2.02	0.499	17.88	594.2
2.25	0.554	16.16	659.7
2.49	0.610	14.75	726.4
2.74	0.665	13.65	792
2.99	0.721	12.68	859
3.23	0.776	11.82	924
3.49	0.832	11.11	991
3.74	0.887	10.47	1056
3.99	0.942	9.91	1122
4.26	0.998	9.42	1188
4.50	1.05	9.00	1250
4.79	1.11	8.57	1322
5.48	1.25	7.73	1489
6.84	1.52	6.52	1810
8.61	1.85	5.54	2203
12.31	2.46	4.42	2929
16.18	3.10	3.71	3692
20.32	3.70	3.27	4406
24.94	4.32	2.94	5144
29.92	4.94	2.70	5883
35.41	5.58	2.50	6645
41.09	6.20	2.36	7383
46.90	6.79	2.24	8086
53.39	7.43	2.13	8848
60.12	8.05	2.05	9586
67.54	8.70	1.97	10360
74.61	9.29	1.90	11063
82.12	9.89	1.85	11777
90.49	10.53	1.80	12539
98.82	11.14	1.75	13266

TABLE 10

Investigator: N. Ahmed

Properties of Media: Sand ; d_s = 0.107 cm; k = 6.91×10^{-6} cm^2;

ϵ = 42.6% ; ϵ_c = 42.6% ; d_g = 0.1075 cm;

d_p = 0.0507 cm; S_v = 69.5 cm^{-1}

Properties of Fluid: $\mu = 0.01559138 \dfrac{\text{dyne-sec}}{cm^2}$; $\rho = 1.0 \dfrac{gm}{cm^3}$

Equation: $\phi = 2.299\, q + 0.30672\, q^2$; S_y = 1.0% ; c = 1.60 ;

d = 2.07×10^{-3} cm.

Equation valid for the range of velocities from 0.00489 cm/sec to 14.96 cm/sec.

ϕ unitless	q cm/sec	H unitless	$N \times 10^4$ unitless
0.01102	0.00489	1498	6.49
0.01654	0.00733	1001	9.73
0.02598	0.0112	675.2	14.87
0.03150	0.0137	544.5	18.19
0.04094	0.0176	429.2	23.37
0.04488	0.0196	379.8	26.0
0.05906	0.0264	275.3	35.1
0.07874	0.0342	218.7	45.4
0.09291	0.0401	187.7	53.2
0.1134	0.0489	154.1	64.9
0.1307	0.0562	134.5	74.6
0.1591	0.0684	110.5	90.8
0.1921	0.0826	91.5	109.7
0.2270	0.0973	77.9	129.2
0.257	0.110	69.0	146.0
0.283	0.121	62.8	160.6
0.336	0.143	53.4	189.9
0.391	0.166	46.1	220.4
0.437	0.185	41.5	245.6

TABLE 10 - Cont'd.

ϕ unitless	q cm/sec	H unitless	N x 10^4 unitless
0.526	0.222	34.7	294.7
0.602	0.253	30.6	335.9
0.709	0.296	26.3	393.0
0.811	0.337	23.2	447.4
0.94	0.388	20.2	515.1
1.08	0.443	17.9	588.2
1.23	0.499	16.1	662.5
1.37	0.554	14.5	735.5
1.52	0.610	13.3	809.9
1.67	0.665	12.3	882.9
1.82	0.721	11.4	957.2
1.97	0.776	10.6	1030
2.13	0.832	10.0	1105
2.28	0.887	9.4	1178
2.44	0.942	8.93	1251
2.60	0.998	8.48	1325
2.76	1.05	8.13	1394
2.93	1.11	7.73	1474
3.36	1.25	6.99	1660
4.21	1.52	5.92	2018
5.31	1.85	5.04	2456
7.52	2.46	4.04	3266
10.08	3.10	3.41	4116
12.71	3.70	3.02	4912
15.67	4.32	2.73	5735
18.85	4.94	2.51	6559
22.39	5.58	2.34	7408
26.05	6.20	2.20	8231
29.76	6.79	2.10	9015
34.02	7.43	2.00	9864
38.39	8.05	1.92	10688
43.22	8.70	1.86	11551
47.83	9.29	1.80	12334
52.73	9.89	1.75	13131
58.21	10.53	1.71	13980
63.66	11.14	1.67	14790
70.10	11.83	1.63	15706
91.51	13.93	1.53	18494
103.01	14.96	1.49	19862

TABLE 11

Investigator: N. Ahmed

Properties of Media: Sand; $d_s = 0.1405$ cm; $k = 1.0 \times 10^{-5}$ cm^2;

$\epsilon = 41.1\%$; $\epsilon_c = 40.8\%$; $d_g = 0.140$ cm;

$d_p = 0.0703$ cm; $S_v = 50.0$ cm^{-1}.

Properties of Fluid: $\mu = 0.01464 \dfrac{\text{dyne-sec}}{\text{cm}^2}$; $\rho = 1.0 \dfrac{\text{gm}}{\text{cm}^3}$

Equation: $\phi = 1.49209\, q + 0.244832\, q^2$; $S_y = 2.5\%$; $c = 1.736$;

$d = 2.4 \times 10^{-3}$ cm.

Equation valid for the range of velocities from 0.0112 cm/sec to 20.14 cm/sec.

ϕ unitless	q cm/sec	H unitless	N x 10^3 unitless
0.0165	0.0112	539.51	1.836
0.0205	0.0137	445.51	2.246
0.0268	0.0176	353.35	2.885
0.0291	0.0196	309.72	3.213
0.0394	0.0264	231.06	4.328
0.0512	0.0342	178.86	5.607
0.0606	0.0401	154.14	6.574
0.0740	0.0489	126.50	8.016
0.0850	0.0562	110.03	9.213
0.1031	0.0684	90.05	11.21
0.125	0.0826	74.89	13.54
0.148	0.0973	63.88	15.95
0.167	0.110	56.40	18.03
0.184	0.121	51.39	19.84
0.219	0.143	43.78	23.44
0.255	0.166	37.83	27.21
0.285	0.185	34.11	30.33
0.344	0.222	28.54	36.39
0.393	0.253	25.09	41.48

TABLE 11 - Cont'd.

ϕ unitless	q cm/sec	H unitless	N x 10^3 unitless
0.463	0.296	21.60	48.52
0.531	0.337	19.11	55.25
0.616	0.388	16.74	63.61
0.709	0.443	14.76	72.62
0.803	0.499	13.19	81.80
0.906	0.554	12.07	90.82
1.000	0.610	10.97	100.0
1.102	0.665	10.17	109.0
1.197	0.721	9.41	118.2
1.300	0.776	8.54	127.2
1.409	0.832	8.32	136.4
1.520	0.887	7.90	145.4
1.622	0.942	7.47	154.4
1.732	0.998	7.11	163.6
1.843	1.05	6.83	172.1
1.961	1.11	6.50	182.0
2.252	1.25	5.89	204.9
2.827	1.52	5.00	249.2
3.598	1.85	4.30	303.3
5.150	2.46	3.48	403.3
6.984	3.10	2.97	508.2
8.882	3.70	2.66	606.6
11.02	4.32	2.41	708.2
13.35	4.94	2.24	809.8
16.08	5.58	2.11	914.8
18.67	6.20	1.99	1016
21.42	6.79	1.90	1113
24.61	7.43	1.82	1218
27.88	8.05	1.76	1320
31.52	8.70	1.70	1426
35.00	9.29	1.66	1523
38.71	9.89	1.61	1621
42.86	10.53	1.58	1726
51.92	11.83	1.52	1939
65.42	13.58	1.45	2226
80.51	15.34	1.40	2515
96.14	17.00	1.36	2787
108.98	18.29	1.33	2998
129.45	20.14	1.30	3302

TABLE 12

Investigator: N. Ahmed

Properties of Media: Sand; $d_s = 0.1992$ cm; $k = 1.69 \times 10^{-5}$ cm^2;

$\epsilon = 40.4\%$; $\epsilon_c = 40.2\%$; $d_g = 0.20$ cm;

$d_p = 0.102$ cm; $S_v = 33.9$ cm^{-1}.

Properties of Fluid: $\mu = 0.01559138 \frac{\text{dyne-sec}}{\text{cm}^2}$; $\rho = 1.0 \frac{\text{gm}}{\text{cm}^3}$.

Equation: $\phi = 0.93837\, q + 0.17931\, q^2$; $S_y = 1.0\%$; $c = 1.92$;

$d = 2.97 \times 10^{-3}$ cm.

Equation valid for the range of velocities from 0.0112 cm/sec to 26.24 cm/sec.

ϕ unitless	q cm/sec	H unitless	$N \times 10^3$ unitless
0.0102	0.0112	454.81	2.133
0.0126	0.0137	373.54	2.610
0.0165	0.0176	296.69	3.353
0.0181	0.0196	262.74	3.734
0.0252	0.0264	201.49	5.029
0.0323	0.0342	153.89	6.515
0.0378	0.0401	131.04	7.639
0.0465	0.0489	108.41	9.315
0.0535	0.0562	94.42	10.71
0.0654	0.0684	77.92	13.03
0.0787	0.0826	64.27	15.73
0.0929	0.0973	54.69	18.53
0.106	0.110	48.83	20.95
0.117	0.121	44.53	23.05
0.138	0.143	37.61	27.24
0.161	0.166	32.57	31.62
0.180	0.185	29.31	35.24
0.218	0.222	24.65	42.29
0.250	0.253	21.77	48.19

TABLE 12 - Cont'd.

ϕ unitless	q cm/sec	H unitless	N x 10^3 unitless
0.294	0.296	18.71	56.39
0.337	0.337	16.54	64.20
0.391	0.388	14.47	73.91
0.452	0.443	12.84	84.39
0.513	0.499	11.48	95.05
0.576	0.554	10.46	105.5
0.638	0.610	9.56	116.2
0.701	0.665	8.84	126.7
0.772	0.721	8.27	137.3
0.835	0.776	7.73	147.8
0.906	0.832	7.30	158.5
0.976	0.887	6.92	169.0
1.047	0.942	6.58	179.4
1.118	0.998	6.26	190.1
1.181	1.05	5.97	200.0
1.260	1.11	5.70	211.4
1.457	1.25	5.19	238.1
1.843	1.52	4.45	289.5
2.354	1.85	3.84	352.4
3.402	2.46	3.14	468.6
4.638	3.10	2.69	590.5
5.929	3.70	2.41	704.8
7.409	4.32	2.21	822.9
9.020	4.94	2.06	941.0
10.82	5.58	1.93	1063
12.72	6.20	1.85	1181
14.64	6.79	1.77	1293
16.88	7.43	1.70	1415
19.18	8.05	1.65	1533
21.74	8.70	1.60	1657
24.20	9.29	1.56	1770
26.82	9.89	1.53	1884
29.77	10.53	1.49	2006
36.20	11.83	1.44	2253
47.45	13.86	1.38	2640
62.06	16.17	1.32	3080
71.76	17.56	1.30	3345
81.39	18.85	1.27	3591
96.24	20.70	1.25	3943
111.42	22.45	1.23	4276
125.98	24.02	1.21	4576
148.05	26.24	1.20	4998

TABLE 13

Investigator: N. Ahmed

Properties of Media: Sand; d_s = 0.258 cm; k = 2.21×10^{-5} cm^2;

ϵ = 40.5%; ϵ_c = 40.7%; d_g = 0.258 cm;

d_p = 0.133 cm; S_v = 26.4 cm^{-1}.

Properties of Fluid: $\mu = 0.0150362 \dfrac{\text{dyne-sec}}{\text{cm}^2}$; $\rho = 1.0 \dfrac{\text{gm}}{\text{cm}^3}$.

Equation: $\phi = 0.69441\, q + 0.165050\, q^2$; S_y = 2.0%; c = 1.727;

d = 3.58×10^{-3} cm.

Equation valid for the range of velocities from 0.0112 cm/sec to 25.50 cm/sec.

ϕ unitless	q cm/sec	H unitless	$N \times 10^3$ unitless
0.0079	0.0112	383.32	2.667
0.0094	0.0137	303.26	3.262
0.0118	0.0176	230.84	4.190
0.0134	0.0196	211.68	4.667
0.0181	0.0264	157.51	6.286
0.0236	0.0342	122.33	8.143
0.0283	0.0401	106.75	9.547
0.0346	0.0489	87.77	11.64
0.0394	0.0562	75.69	13.38
0.0480	0.0684	62.23	16.29
0.0583	0.0826	51.83	19.67
0.0693	0.0973	44.40	23.17
0.0780	0.110	39.10	26.19
0.0866	0.121	35.88	28.81
0.1024	0.143	30.38	34.05
0.120	0.166	26.41	39.52
0.134	0.185	23.75	44.05
0.162	0.222	19.94	52.86
0.186	0.253	17.62	60.24
0.220	0.296	15.23	70.48

TABLE 13 - Cont'd.

ϕ unitless	q cm/sec	H unitless	N x 10^3 unitless
0.252	0.337	13.46	80.24
0.294	0.388	11.85	92.38
0.339	0.443	10.47	105.47
0.387	0.499	9.43	118.81
0.435	0.554	8.59	131.90
0.484	0.610	7.89	145.2
0.534	0.665	7.32	158.3
0.585	0.721	6.82	171.7
0.637	0.776	6.42	184.5
0.691	0.832	6.05	198.1
0.745	0.887	5.74	211.2
0.799	0.942	5.46	224.3
0.856	0.998	5.22	237.6
0.910	1.05	5.01	250.0
0.973	1.11	4.79	264.3
1.12	1.25	4.34	297.6
1.43	1.52	3.76	361.9
1.85	1.85	3.28	440.5
2.70	2.46	2.70	585.7
3.73	3.10	2.36	738.1
4.82	3.70	2.13	880.9
6.07	4.32	1.97	1029
7.45	4.94	1.85	1176
9.00	5.58	1.75	1329
10.64	6.20	1.68	1476
12.31	6.79	1.62	1617
14.26	7.43	1.56	1769
16.27	8.05	1.52	1917
18.52	8.70	1.49	2071
20.68	9.29	1.45	2212
22.99	9.89	1.42	2355
25.59	10.53	1.40	2507
31.29	11.83	1.36	2817
39.84	13.58	1.31	3233
49.46	15.34	1.28	3652
59.47	17.00	1.25	4048
67.87	18.29	1.23	4355
80.93	20.14	1.21	4795
96.54	22.18	1.19	5281
111.84	24.02	1.17	5719
124.96	25.50	1.17	6071

TABLE 14

Investigator: H. V. Allen

Properties of Media: Granular Absorbents; $d_s = 0.0855$ cm;

$k = 8.6 \times 10^{-6}$ cm^2 .

Properties of Fluid: $\mu = 0.0091 \dfrac{\text{dyne-sec}}{cm^2}$; $\rho = 0.78$ gm/cm^3 (Naptha).

Equation: $\phi = 1.47 + 0.142\, q^2$; $S_y = 3.3\%$; $c = 3.65$; $d = 1.53 \times 10^{-3}$ cm.

Equation valid for the range of velocities from 0.156 cm/sec to 2.21 cm/sec.

ϕ unitless	q cm/sec	H unitless	$N \times 10^3$ unitless
0.233	0.156	53.1	20.5
0.482	0.286	32.2	37.5
0.569	0.367	23.06	48.1
0.628	0.408	20.60	53.5
0.934	0.619	13.32	81.2
1.080	0.687	12.5	90.1
1.34	0.856	10.02	112.3
1.52	0.972	8.81	127.5
1.75	1.09	8.07	142.9
1.90	1.22	6.99	160.0
2.13	1.33	6.59	174.4
2.45	1.50	5.95	196.7
2.92	1.70	5.53	222.9
3.18	1.87	4.985	245.2
3.71	2.04	4.88	267.5
4.09	2.21	4.59	289.8

TABLE 15

Investigator: F. C. Blake

Properties of Media: Glass Beads; $d_s = 0.32$ cm;

$k = 6.7 \times 10^{-5}\ cm^2$.

Properties of Fluid: $\mu = 0.01 \dfrac{\text{dyne-sec}}{cm^2}$; $\rho = 1.0 \dfrac{gm}{cm^3}$.

Equation: $\phi = 0.149\, q + 0.0623\, q^2$; $S_y = 1.6\%$; $c = 4$;

$d = 4.1 \times 10^{-3}$ cm .

Equation valid for the range of velocities from 0.814 cm/sec to 7.18 cm/sec.

ϕ unitless	q cm/sec	$H \times 10^3$ unitless	$N \times 10$ unitless
0.163	0.814	3956	3.34
0.281	1.22	3037	5.00
0.463	1.76	2405	7.22
0.614	2.16	2117	8.86
0.849	2.71	1860	11.11
1.246	3.52	1618	14.43
2.176	4.81	1513	19.72
3.217	6.10	1391	25.01
4.312	7.18	1346	29.44

TABLE 16

Investigator: L. E. Brownell

Properties of Media: Glass Beads; $d_s = 0.53$ cm ; $\epsilon = 41.2\%$;

$k = 1.5 \times 10^{-4}$ cm^2 .

Properties of Fluid: $\mu = 0.00955 \dfrac{\text{dyne-sec}}{\text{cm}^2}$; $\rho = 1.0 \dfrac{\text{gm}}{\text{cm}^3}$.

Equation: $\phi = 0.0647q + 0.0183\, q^2$; $S_y = 1.4\%$; $c = 20.7$;

$d = 2.7 \times 10^{-3}$ cm .

Equation valid for the range of velocities from 3.41 cm/sec to

12.3 cm/sec.

ϕ unitless	q cm/sec	H unitless	N x 10 unitless
0.424	3.41	2.00	9.64
0.542	3.93	1.92	11.11
0.705	4.60	1.83	13.01
0.833	5.15	1.72	14.56
1.04	6.00	1.58	16.96
1.27	6.82	1.50	19.28
1.60	7.67	1.49	21.68
1.82	8.46	1.39	23.92
2.18	9.44	1.34	26.69
2.70	10.4	1.37	29.40
3.03	11.2	1.32	31.66
3.53	12.3	1.28	34.77

TABLE 17

Investigator: L. E. Brownell

Properties of Media: Nickel Saddles; $d_s = 0.334$ cm ; $\epsilon = 93.1\%$;

$k = 1.12 \times 10^{-4}$ cm^2 .

Properties of Fluid: $\mu = 0.00977 \dfrac{\text{dyne-sec}}{\text{cm}^2}$; $\rho = 1.0 \dfrac{\text{gm}}{\text{cm}^3}$.

Equation: $\phi = 0.08903\, q + 0.02188\, q^2$; $S_y = 5.0\%$; $c = 19.3$;

$d = 2.4 \times 10^{-3}$ cm .

Equation valid for the range of velocities from 5.85 cm/sec to 24.5 cm/sec.

ϕ unitless	q cm/sec	H unitless	N unitless
1.09	5.85	1.45	1.44
1.30	6.66	1.33	1.64
2.06	8.22	1.39	2.02
2.93	9.93	1.35	2.44
4.56	13.8	1.09	3.39
6.46	16.0	1.15	3.93
7.61	17.9	1.08	4.40
8.94	19.7	1.05	4.84
13.0	24.5	0.98	6.02

TABLE 18

Investigator: G. H. Fancher

Properties of Media: 20-30 Ottawa Sand; $d_s = 0.07$ cm (estimated)

$\epsilon = 34.5\%$; $k = 8.2 \times 10^{-7}\ cm^2$.

Properties of Fluid: $\mu = 0.0136\ \frac{dyne\text{-}sec}{cm^2}$; $\rho = 1.0\ \frac{gm}{cm^3}$.

Equation: $\phi = 16.6\ q + 7.96\ q^2$; $S_y = 4.1\%$; $c = 0.02$;

$d = 6.4 \times 10^{-3}$ cm .

Equation valid for the range of velocities from 0.069 cm/sec to

0.855 cm/sec.

ϕ unitless	q cm/sec	H unitless	$N \times 10^3$ unitless
1.22	0.069	31.92	32.47
1.64	0.0896	25.74	42.16
2.74	0.166	12.47	78.12
6.32	0.331	7.24	155.76
9.76	0.48	5.32	225.9
12.4	0.606	4.24	285.2
16.9	0.731	3.97	344.0
20.2	0.855	3.47	402.4

TABLE 19

Investigator: P. H. Forchheimer

Properties of Media: Sand; $d_s = 0.5$ cm ; $k = 2.30 \times 10^{-3}$ cm^2.

Properties of Fluid: $\mu = 0.0091 \dfrac{\text{dyne-sec}}{\text{cm}^2}$; $\rho = 1.0 \dfrac{\text{gm}}{\text{cm}^3}$.

Equation: $\phi = 0.00408\, q + 0.0005\, q^2$; $S_y = 2.2\%$; $c = 1837$;

$d = 1.1 \times 10^{-3}$ cm .

Equation valid for the range of velocities from 0.116 cm/sec to 10.8 cm/sec.

ϕ unitless	q cm/sec	H unitless	$N \times 10^3$ unitless
0.0005	0.116	73.42	14.02
0.0010	0.243	33.60	29.37
0.0020	0.463	18.49	55.97
0.0040	0.891	9.99	107.7
0.0060	1.300	7.04	157.1
0.0080	1.64	5.90	198.2
0.010	2.00	4.96	241.8
0.015	2.75	3.93	332.4
0.020	3.47	3.29	419.5
0.030	4.63	2.77	559.5
0.050	6.48	2.36	783.3
0.100	10.80	1.70	1305.5

TABLE 20

Investigator: P. H. Forchheimer

Properties of Media: Sand; $d_s = 0.3$ cm ; $k = 7.6 \times 10^{-4}$ cm^2 .

Properties of Fluid: $\mu = 0.0091 \dfrac{\text{dyne-sec}}{\text{cm}^2}$; $\rho = 1.0 \dfrac{\text{gm}}{\text{cm}^3}$;

Equation: $\phi = 0.01225\, q + 0.00092\, q^2$; $S_y = 2.1\%$; $c = 1612$;

$d = 0.7 \times 10^{-3}$ cm .

Equation valid for the range of velocities from 0.0405 cm/sec to 5.73 cm/sec.

ϕ unitless	q cm/sec	H unitless	$N \times 10^3$ unitless
0.0005	0.0405	33.75	31.15
0.001	0.0810	16.87	62.31
0.002	0.162	8.45	124.6
0.004	0.312	4.55	240.0
0.006	0.475	2.94	365.4
0.008	0.625	2.27	480.8
0.010	0.775	1.84	596.2
0.015	1.13	1.30	869.2
0.020	1.47	1.02	1130.8
0.030	2.14	0.725	1646
0.050	3.24	0.527	2492
0.10	5.73	0.337	4408

TABLE 21

Investigator: C. E. Kirkham

Properties of Media: Marble ; d_s = 1.6 cm ; $k = 1.197 \times 10^{-3}$ cm^2;

Properties of Fluid: $\mu = 0.010494 \ \frac{\text{dyne-sec}}{cm^2}$; $\rho = 0.99857 \ \frac{gm}{cm^3}$.

Equation: $\phi = 0.0089463\, q + 0.011685\, q^2$; $S_y = 4.1\%$;

$c = 6.36$; $d = 13.7 \times 10^{-3}$ cm .

Equation valid for the range of velocities from 0.0610 cm/sec to

9.6317 cm/sec.

ϕ unitless	q cm/sec	H unitless	$N \times 10^3$ unitless
0.000496	0.0610	11.74	79.52
0.000615	0.0762	9.05	99.34
0.000711	0.0872	7.99	113.68
0.000851	0.1006	7.19	131.15
0.00105	0.1219	6.04	158.91
0.00138	0.1524	5.08	198.7
0.00202	0.2033	4.17	265.0
0.00355	0.3048	3.27	397.3
0.00540	0.4054	2.81	528.5
0.00995	0.6096	2.29	794.7
0.0140	0.7620	2.06	993.4
0.0173	0.8717	1.95	1136
0.0224	1.0058	1.89	1311
0.0297	1.2192	1.71	1589
0.0438	1.5240	1.61	1987
0.0726	2.033	1.50	2650
0.146	3.048	1.34	3973
0.243	4.0538	1.26	5285
0.502	6.0960	1.15	7947
0.741	7.6200	1.09	9934
0.944	8.7173	1.06	11364
1.148	9.6317	1.06	12556

TABLE 22

Investigator: E. Lindquist

Properties of Media: Sand; $d_s = 0.492$ cm ; $\epsilon = 38\%$;

$k = 1.38 \times 10^{-4}$ cm^2 .

Properties of Fluid: $\mu = 0.00914 \dfrac{\text{dyne-sec}}{\text{cm}^2}$; $\rho = 1.0 \dfrac{\text{gm}}{\text{cm}^3}$.

Equation: $\phi = 0.0674\, q + 0.0368\, q^2$; $S_y = 3.0\%$; $c = 5.57$;

$d = 5 \times 10^{-3}$ cm .

Equation valid for the range of velocities from 0.196 cm/sec to 4.60 cm/sec.

ϕ unitless	q cm/sec	H unitless	$N \times 10^3$ unitless
0.015	0.196	10.67	107.22
0.045	0.532	4.34	291.03
0.070	0.742	3.47	405.9
0.120	1.16	2.44	634.6
0.185	1.51	2.22	826.0
0.28	2.00	1.91	1094
0.41	2.55	1.72	1395
0.52	2.95	1.63	1614
0.63	3.30	1.58	1805
0.75	3.70	1.50	2024
0.90	4.06	1.49	2221
1.10	4.60	1.42	2516

TABLE 23

Investigator: E. Lindquist

Properties of Media: Sand ; $d_s = 1.05$ mm ; $\epsilon = 38\%$;

$k = 8 \times 10^{-6}$ cm^2 .

Properties of Fluid: $\mu = 0.00914 \dfrac{\text{dyne-sec}}{\text{cm}^2}$; $\rho = 1.0 \dfrac{\text{gm}}{\text{cm}^3}$.

Equation: $\phi = 1.164\, q + 0.2928\, q^2$; $c = 1.51$; $d = 2.3 \times 10^{-3}$ cm ;

$S_y = 4.5\%$.

Equation valid for the range of velocities from 0.042 cm/sec to 1.02 cm/sec.

ϕ unitless	q cm/sec	H unitless	N x 10^3 unitless
0.045	0.042	87.11	10.57
0.070	0.062	62.11	15.60
0.20	0.155	28.39	39.00
0.31	0.238	18.66	59.89
0.61	0.462	9.739	116.26
0.70	0.504	9.389	126.83
0.81	0.616	7.272	155.01
0.94	0.700	6.536	176.15
1.05	0.756	6.260	190.2
1.35	0.952	5.075	239.6
1.48	1.02	4.846	256.7

TABLE 24

Investigator: F. Mobasheri

Properties of Media: Sand; d_s = 0.5 cm ; k = 4.94 x 10^{-5} cm^2 .

Properties of Fluid: $\mu = 0.00914 \dfrac{\text{dyne-sec}}{\text{cm}^2}$; $\rho = 1.0 \dfrac{\text{gm}}{\text{cm}^3}$.

Equation: $\phi = 0.189\, q + 0.137\, q^2$; c = 1.1 ; d = 6.6 x 10^{-3} cm ;

S_y = 6.5% .

Equation valid for the range of velocities from 0.109 cm/sec to 5.53 cm/sec.

ϕ unitless	q cm/sec	H unitless	N x 10^2 unitless
0.022	0.109	13.17	7.87
0.022	0.117	11.44	8.45
0.028	0.136	10.78	9.82
0.038	0.178	8.54	12.85
0.040	0.194	7.58	14.01
0.046	0.218	6.90	15.74
0.056	0.287	4.84	20.72
0.058	0.300	4.59	21.66
0.074	0.350	4.30	25.27
0.088	0.408	3.76	29.46
0.108	0.458	3.73	33.07
0.130	0.518	3.45	37.40
0.146	0.559	3.66	40.36
0.176	0.621	3.25	44.84
0.186	0.646	3.17	46.65
0.212	0.722	2.90	52.14
0.244	0.777	2.88	56.11
0.280	0.877	2.59	63.33
0.330	1.00	2.35	72.21
0.430	1.182	2.19	85.35
0.544	1.37	2.18	98.93
0.786	1.69	1.96	122.0
1.14	2.15	1.76	155.3

TABLE 24 - Cont'd.

ϕ unitless	q cm/sec	H unitless	N x 10^2 unitless
1.58	2.68	1.57	193.5
1.83	2.97	1.48	214.5
2.27	3.40	1.40	245.5
3.20	4.19	1.30	302.6
3.69	4.57	1.26	330.0
4.24	4.96	1.23	358.2
4.68	5.27	1.20	380.5
5.11	5.53	1.19	399.3

TABLE 25

Investigator: D. K. Sunada

Properties of Media: Glass Spheres; $d_s = 0.300 \pm 0.005$ cm ;

$\epsilon = 37.1\%$; $k = 6.45 \times 10^{-5}$ cm^2 .

Properties of Fluid: $\mu = 0.0091 \frac{\text{dyne-sec}}{\text{cm}^2}$; $\rho = 1.0 \frac{\text{gm}}{\text{cm}^3}$.

Equation: $\phi = 0.145\, q + 0.0648\, q^2$; $S_y = 4.4\%$; $c = 3.8$;

$d = 4.1 \times 10^{-3}$ cm .

Equation valid for the range of velocities from 0.01 cm/sec to 15 cm/sec.

ϕ unitless	q cm/sec	H unitless	$N \times 10^3$ unitless
0.0015	0.011	189.5	4.956
0.00232	0.0175	114.4	7.88
0.00400	0.0243	103.6	10.95
0.00440	0.0335	60.04	15.09
0.00575	0.0422	49.37	19.01
0.00716	0.0509	42.25	22.93
0.00814	0.0596	35.05	26.85
0.01070	0.0789	26.25	35.55
0.0136	0.0944	23.33	42.53
0.0165	0.118	18.14	53.16
0.0192	0.135	16.12	60.82
0.0250	0.172	12.91	77.49
0.0275	0.187	12.00	84.25
0.0312	0.208	11.01	93.71
0.0350	0.228	10.29	102.7
0.0400	0.248	9.94	111.7
0.0460	0.288	8.48	129.8
0.0475	0.298	8.18	134.3
0.0500	0.308	8.05	138.8
0.0537	0.330	7.54	148.7
0.0600	0.368	6.77	165.8
0.0664	0.388	6.74	174.8

TABLE 25 - Cont'd.

ϕ unitless	q cm/sec	H unitless	N x 10^3 unitless
0.0725	0.428	6.05	192.8
0.0537	0.330	7.54	148.7
0.0555	0.338	7.43	152.3
0.0587	0.356	7.08	160.4
0.0625	0.376	6.76	169.4
0.0700	0.408	6.43	183.8
0.0348	0.215	11.51	96.9
0.0406	0.251	9.85	113.1
0.0475	0.300	8.07	135.2
0.0614	0.365	7.06	164.5
0.0540	0.329	7.64	148.2
0.0689	0.408	6.34	183.8
0.0760	0.445	5.87	200.5
0.0843	0.485	5.48	218.5
0.0930	0.512	5.43	230.7
0.101	0.561	4.90	252.8
0.1095	0.600	4.65	270.3
0.114	0.640	4.25	288.4
0.1205	0.680	3.99	306.4
0.1525	0.758	4.05	341.5
0.167	0.838	3.64	377.6
0.190	0.918	3.48	413.6
0.210	0.995	3.24	448.3
0.232	1.09	2.98	491.1
0.260	1.15	3.00	518.1
0.283	1.23	2.86	554.2
0.313	1.30	2.83	585.7
0.340	1.38	2.73	621.8
0.363	1.46	2.60	657.8
0.373	1.54	2.40	693.8
0.461	1.720	2.38	774.9
0.525	1.890	2.25	851.5
0.595	2.03	2.21	914.6
0.674	2.19	2.15	986.7
0.756	2.35	2.09	1059
0.875	2.58	2.01	1162
1.00	2.82	1.92	1271
1.17	3.14	1.81	1415

TABLE 25 - Cont'd.

ϕ unitless	q cm/sec	H unitless	N x 10^3 unitless
1.44	3.52	1.78	1586
1.65	3.92	1.64	1766
2.08	4.50	1.57	2027
2.43	5.05	1.46	2275
2.78	5.48	1.41	2469
3.50	6.26	1.37	2820
4.35	7.18	1.29	3235
5.56	8.38	1.21	3776
6.15	8.80	1.21	3965
7.00	9.38	1.22	4226
7.89	10.1	1.18	4551
8.58	10.4	1.21	4686
9.46	11.0	1.19	4956
10.60	11.80	1.16	5316
12.00	12.55	1.16	5654
13.10	13.2	1.15	5947
14.6	14.0	1.14	6308